Clim. Past Discuss., https://doi.org/10.5194/cp-2018-119
Manuscript under review for journal Clim. Past
Discussion started: 20 September 2018

Climate of the Past Discussions
Open Access
EGU

Rapid recovery of Ediacaran oceans in the aftermath of the Marinoan glaciation

Anthony Dosseto[1,*], Holly L. Taylor[1], Juraj Farkaš[2,3], Grant M. Cox[2], Andrew Kingston[4], Andrew Lorrey[5], Alexander J. Corrick[2] and Bing Shen[6]

[1] Wollongong Isotope Geochronology Laboratory, School of Earth & Environmental Sciences. University of Wollongong. Wollongong, NSW, Australia

[2] Department of Earth Sciences. University of Adelaide. Adelaide, SA, Australia

[3] Department of Environmental Geosciences, Czech University of Life Sciences, Prague, Czech Republic

[4] National Institute of Water and Atmospheric Research. Wellington, New Zealand

[5] National Institute of Water and Atmospheric Research. Auckland, New Zealand

[6] Ministry of Education Key Laboratory of Orogenic Belts and Crustal Evolution, School of Earth and Space Sciences, Peking University, Beijing 100871, People's Republic of China

** corresponding author: tonyd@uow.edu.au*

Clim. Past Discuss., https://doi.org/10.5194/cp-2018-119
Manuscript under review for journal Clim. Past
Discussion started: 20 September 2018

Climate of the Past Discussions
Open Access
EGU

ABSTRACT

The termination of Cryogenian glaciations would have undoubtedly impacted the chemistry of Neoproterozoic oceans, with possible consequences for life; but the extent and duration of this impact are poorly constrained. In this study, we use the lithium (Li) isotope composition of Ediacaran cap dolostones from South Australia (Nuccaleena Formation) and China (Doushantuo Fm) to investigate changes in ocean chemistry that followed the Marinoan deglaciation. The effect of diagenesis was evaluated and while the Nuccaleena Fm is likely to have preserved the primary composition of cap dolostone deposition, the offset in Li isotope ratios observed for the Doushantuo Fm could possibly reflect partial overprinting by diagenetic fluids. The Li isotope composition of Ediacaran seawater was estimated and we suggest it was similar to that of late Cenozoic oceans for most of the cap dolostone deposition. Using a box model for the oceanic Li cycle, we show that at the onset of deglaciation, the supply of riverine Li to the oceans was up to 50 times the modern flux. The modelled riverine Li isotope composition suggests that continents resembled modern high-latitude regions during this time. This episode was short-lived (up to 1 Myr) and the subsequent supply of riverine Li was similar to modern conditions, both in flux and isotope composition, for the whole duration of cap dolostone deposition. These results suggest that Ediacaran oceans and continents rapidly recovered from the Marinoan glaciation to reach environmental conditions similar to the late Cenozoic. From the standpoint of the Li oceanic budget, the Ediacaran oceans in which complex lifeforms emerged may have not been that different from our modern oceans.

Clim. Past Discuss., https://doi.org/10.5194/cp-2018-119
Manuscript under review for journal Clim. Past
Discussion started: 20 September 2018

1. Introduction

The Neoproterozoic era (1,000-542 Myr ago) is characterised by major environmental changes including global glaciations (Hoffman et al., 2017), a second major increase in atmospheric oxygen (Och and Shields-Zhou, 2012;Sahoo et al., 2016;Scott et al., 2008) and the radiation of complex lifeforms (Knoll and Carroll, 1999). Biomarkers suggest that the first metazoans emerged sometime in between the Sturtian and Marinoan glaciations (Love et al., 2009), with algae replacing phototropic bacteria as the top marine primary producer between 659 and 650 Ma (Brocks et al., 2017). This shift has been suggested as resulting from a massive supply of nutrients to the oceans at the end of the Sturtian glaciation (Brocks et al., 2017). The end of the Marinoan glaciation could have triggered another major leap in evolution, since it is followed by the appearance of centimetre-scale macroalgae and a significant increase in metazoan complexity and diversity (Yuan et al., 2011;Yin et al., 2007;Yin et al., 2015).

The termination of the Marinoan glaciation is capped by the occurrence of dolostones, termed “cap carbonates” (Rose and Maloof, 2010;Hoffman et al., 2017). These unique formations are useful archives of changes in ocean chemistry that took place following the Marinoan glaciation. For instance, their boron isotopic composition suggests ocean acidification (Ohnemueller et al., 2014;Kasemann et al., 2005) while triple oxygen isotopes show that atmospheric carbon dioxide levels were at their highest levels in the past 750 million years (Bao et al., 2008). Calcium (Ca) isotopes show that the Ca supply to the oceans would have been 14 to 140 times greater than the modern flux, and this was interpreted as a large pulse in continental weathering (Kasemann et al., 2005). Zinc and cadmium isotopes hint at a rapid resumption of primary productivity (Kunzmann et al., 2013;John et al., 2017). Huang et al. (2016) have also used magnesium isotopes (δ^{26}Mg) to suggest that a rapid pulse of continental weathering took place prior to the end of the Marinoan glaciation, and subsided following cap carbonate deposition. While their results provide some important insights on

Clim. Past Discuss., https://doi.org/10.5194/cp-2018-119
Manuscript under review for journal Clim. Past
Discussion started: 20 September 2018

environmental changes associated with large Neoproterozoic glaciations, because they focus on siliclastic sediments the changes observed could reflect changes in the provenance of sediments mobilised by erosion. For instance, the pulse in weathering inferred from high $\delta^{26}Mg$ values at the end of the Marinoan glaciation could reflect preferential erosion of sediments from continental regions characterised by higher weathering intensity instead of a globally more intense continental weathering. Furthermore, while Ca isotopes suggest a large element flux from the continents, there is the need for testing this hypothesis with an unequivocal proxy for silicate weathering. In order to fill this gap, we use the lithium (Li) isotopic composition of Ediacaran cap carbonates to investigate possible changes in riverine inputs to the ocean that reflect continental weathering.

Lithium isotopes (^{7}Li and ^{6}Li) fractionate during the formation of secondary minerals, with ^{6}Li being preferentially incorporated into the solid, and thus have been used as a proxy for silicate weathering (Burton and Vigier, 2011;Wimpenny et al., 2010;Pistiner and Henderson, 2003;Verney-Carron et al., 2011;Decarreau et al., 2012). For instance, the Li isotopic composition (noted $\delta^{7}Li$) of river waters records the extent of secondary mineral formation at the catchment scale, where low $\delta^{7}Li$ values are diagnostic of intense weathering (Millot et al., 2010;Vigier et al., 2009). The Li isotopic composition of marine carbonates can then be used to investigate how the riverine Li supply to the oceans has varied over time, reflecting changes in continental weathering (Vigier and Goddéris, 2015;Li and West, 2014;Misra and Froelich, 2012;Wanner et al., 2014;Pogge von Strandmann et al., 2013;Lechler et al., 2015;Pogge von Strandmann et al., 2017a). For instance, the increase in $\delta^{7}Li$ values in foraminifera throughout the Cenozoic has been interpreted as a consequence of the Himalayan and Andean orogeneses, due to either a shift in continental weathering regime from transport-limited, deeply weathered lowlands, to weathering-limited, poorly weathered steep terranes (Misra and Froelich, 2012;Wanner et al., 2014;Vigier and Goddéris, 2015); or an increase in

Clim. Past Discuss., https://doi.org/10.5194/cp-2018-119
Manuscript under review for journal Clim. Past
Discussion started: 20 September 2018

submarine "reverse" weathering of authigenic clays (Li and West, 2014). For the former, it has been proposed that the shift in continental weathering is represented either by a transition from congruent to incongruent dissolution (Misra and Froelich, 2012), a decrease in weathering intensity and increase in river suspended load (Wanner et al., 2014) or a decrease in Li storage in secondary phases (Vigier and Goddéris, 2015). The δ^7Li composition of calcite in chalk was also used to evidence a large weathering pulse in the wake of the Ocean Anoxic Event 2 (OAE2), which could have contributed to a rapid recovery from the greenhouse state associated with the OAE2 (Pogge von Strandmann et al., 2013). The δ^7Li composition of Ordovician bulk carbonates, brachiopods and shales showed that silicate weathering intensity was reduced during the Hirnantian glaciation, resulting in inhibited CO_2 drawdown which could have facilitated deglaciation (Pogge von Strandmann et al., 2017a).

In this study, Li isotope compositions were measured on two Marinoan cap carbonate formations from Australia and China: the Nuccaleena Formation (Fm) and Member I of the Doushantuo Fm, respectively. In combination with the recent determination of Li isotope fractionation during Ca-Mg carbonate precipitation (Taylor et al., 2018), results are used to model changes in the Li budget of Ediacaran oceans.

2. Study area

The Doushantuo Fm is part of the Yantgze block in China (Figure 1a), and was deposited in a passive-margin setting (Jiang et al., 2011). We focused on the Lower Dolomite Member (or Member I) which refers to ~5 m of massive and laminated dolomite beds at the base of the Doushantuo Fm (Chen et al., 2004). Thirty-one samples were collected from core 14ZK at Daotuo village in Songtao county (28.131750 N, 108.892444 E WGS84), where the cap dolostone is mainly composed of microcrystalline dolomite and dolomicrite with sheet-crack structures (Huang et al., 2016).

Clim. Past Discuss., https://doi.org/10.5194/cp-2018-119
Manuscript under review for journal Clim. Past
Discussion started: 20 September 2018

The Nuccaleena Fm is located in South Australia and is part of the Adelaide Rift Complex (Preiss, 1987), where Neoproterozoic sediments accumulated as a result of a succession of rift and thermal subsidence phases (Jenkins, 1990). The Nuccaleena Fm was sampled at Elatina Creek (31.357989 S, 138.617613 E WGS84; Figure 1b). It is underlain by glacial diamectite and siltstone deposits of the Elatina Fm and is overlain by interbedded shales and sandstones of the Brachina Fm. At Elatina Ck, we measured a thickness for the Nuccaleena Fm of 4.2 m, in agreement with Raub (2008). Twenty-eight samples were collected in total: three samples in the transition zone between the Elatina and Nuccaleena Fms (EC-1 to EC-3), 21 in the Nuccaleena Fm proper and four in the transition zone between the Nuccaleena and Brachina Fms. The total thickness of section sampled was 6.75 m from the lowest to the highest sample.

Font et al. (2010) suggested that the Nuccaleena Formation was deposited in only a few 100's of kyr; however, there are no radiometric dates that constrain the duration of deposition of this formation. Condon et al. (2005) were able to bracket the duration of the Lower Dolomite Member using ash beds, and it was estimated between 1.7 and 3.8 Myr. Numerical simulations have suggested a duration for deglaciation of only 2 kyr (Hyde et al., 2000). Cap carbonate deposition was proposed to have continued for several tens of thousands years afterward (Creveling and Mitrovica, 2014), although this is significantly shorter than the proposed duration by Condon et al. (2005). Both sections were correlated assuming synchronicity of deposition and considering a total thickness of 5 and 4.2 m for the Lower Dolomite Member in core 14ZK and the Nuccaleena Fm at Elatina Ck (Raub et al., 2007), respectively.

3. Methods

3.1. Mineralogy

Clim. Past Discuss., https://doi.org/10.5194/cp-2018-119
Manuscript under review for journal Clim. Past
Discussion started: 20 September 2018

Mineralogical compositions were determined on bulk samples of the Nuccaleen Fm at University of Wollongong. This was undertaken by powder X-ray diffraction (PXRD) of finely ground aliquots performed on a PANalytical X'Pert PRO diffractometer outfitted with a Co-target tube (operated at 40 kV and 40 mA), a high-speed Scientific X´Celerator detector, 0.5° antiscattering and divergence slits, spinner stage, primary and secondary soller, as well as an automatic sample changer. Samples were finely ground by hand using a mortar and pestle prior to analysis and were loaded in a random orientation using the top loading technique. The samples were analyzed over the range 4 – 85° 2θ with a step size of 0.008° 2θ and a count time of 40 seconds/step. Mineral quantification was obtained by Rietveld Refinement of the XRD patterns using the PANalytical X'Pert HighScore Plus Software and its implemented pdf-2 database.

3.2. Oxygen and carbon isotopic compositions

Ground bulk samples were prepared and analysed for oxygen and carbon isotopes at the National Institute of Water and Atmospheric Research. Each sample was reacted with 3 drops of H_3PO_4 at 75°C in a Kiel automated individual carbonate reaction device coupled with a mass spectrometer. Either a Kiel III coupled to MAT 252 mass spectrometer or a Kiel IV coupled with MAT 253 mass spectrometer were used to derive $^{18}O/^{16}O$ and $^{13}C/^{12}C$ measurements. All values are reported relative to Vienna Pee Dee Belemnite (VPDB), where $\delta^{13}C$ has a value of +1.95‰ and $\delta^{18}O$ has a value of -2.20 ‰ for NBS19 calcite. Internal precision of measurements is 0.02-0.08 ‰ for $\delta^{18}O$ and 0.01-0.06 ‰ for $\delta^{13}C$, external precision is 0.03‰ for $\delta^{18}O$ and 0.02‰ for $\delta^{13}C$, relative to VPDB.

Clim. Past Discuss., https://doi.org/10.5194/cp-2018-119
Manuscript under review for journal Clim. Past
Discussion started: 20 September 2018

169 *3.3. Lithium isotopic compositions and element concentrations*

170 Sample preparation for Li isotope and trace element concentration measurement was
171 undertaken in a Class 100 cleanroom at the Wollongong Isotope Geochronology Laboratory,
172 University of Wollongong. Because dolostones contain a significant proportion of siliclastic
173 material, samples were leached following the protocol recently developed by Taylor et al.
174 (2018): one gram of ground rock was weighed and leached with 0.05M HCl at room
175 temperature for 1 hr. Samples were then centrifuged and the supernatant was weighed, dried
176 down and re-dissolved in a weighed amount of 0.3M HNO_3. Aliquots of solution were taken,
177 weighed and diluted 100 times for Ti, Mn, Rb, Sr and Li concentration determinations and
178 10,000 times for Mg, Ca and Al concentrations. The remainder was dried down, and re-
179 dissolved in 1M HCl. A volume of solution equivalent to ~60 ng of Li was processed for cation
180 exchange chromatography procedure, as described in Balter and Vigier (2014); calibration of
181 each column was assessed using seawater (Taylor et al., 2018).

182 Element concentrations were determined by single collector ICP-MS (Inductively
183 Coupled Plasma Mass Spectrometry) on a ThermoFisher iCAP-Q at the Wollongong Isotope
184 Geochronology Laboratory, University of Wollongong. Samples were introduced in 0.3M
185 HNO_3 using a concentric nebuliser and cyclonic spray chamber. Standard nickel cones were
186 used. Concentrations were calculated using an external calibration curve, established by
187 analysing seven calibration standards (Inorganic Ventures 71A) with concentrations ranging
188 from 0.05 to 100 ppb. Instrument blank correction was applied during analysis. Drift correction
189 was performed using element standard 71D from Inorganic Ventures.

190 Lithium isotope ratios were measured by MC ICP-MS (Multi Collector Inductively
191 Coupled Plasma Mass Spectrometry) on a ThermoFisher Neptune Plus at the Wollongong
192 Isotope Geochronology Laboratory, University of Wollongong. A 30 ppb solution of IRMM-
193 16 Li isotopic standard was used at the start of each session to tune the instrument. An intensity

Clim. Past Discuss., https://doi.org/10.5194/cp-2018-119
Manuscript under review for journal Clim. Past
Discussion started: 20 September 2018

of ~1 V was routinely obtained for ^{7}Li, while the background ^{7}Li intensity was between 5-30 mV. During analysis, standard bracketing, using IRMM-16 as the primary standard, was applied to correct the measured $^{7}Li/^{6}Li$ for mass bias (Flesch et al., 1973). The accuracy of analysis was assessed using synthetic solutions Li6-N and Li7-N as secondary standards (Carignan et al., 2007) every 6 samples. Before each standard and sample, the instrument blank was measured and subtracted from each isotope. The $^{7}Li/^{6}Li$ ratios are expressed as $\delta^{7}Li$ values using L-SVEC to normalize the isotopic ratio (Carignan et al., 2007).

4. Results

For the Nuccaleena Fm, most samples show dolomite contents between 70 and 83 wt. % (Figure 2). However, four samples (two at the bottom, two at the top of the section) show values as low as 33 wt. % (Table 1). These samples are also characterised by higher concentrations of quartz (up to 32 wt. %) or muscovite (up to 21 wt. %) (Figure 2). They are derived from the Elatina-Nuccaleena and Nuccaleena-Brachina transitions; thus these mineralogical compositions likely reflect waning detrital input to the Ediacaran ocean at the onset of cap carbonate formation, and an increasing siliclastic contribution at its end, eventually dominated by siltstones of the Brachina Fm. Other minerals present are calcite (≤17 wt. %), ankerite and albite (both ≤11 wt. %), chlorite (≤6 wt. %) and kaolinite (≤3 wt. %) (Table 1). Oxygen ($\delta^{18}O$) and carbon ($\delta^{13}C$) isotope compositions range from -8.90 to -6.29 ‰ and from -3.19 to -1.06 ‰, respectively (Table 2). These values are similar to previously published data on the Nuccaleena Fm for the same section (Rose and Maloof, 2010) and at two other locations (Kunzmann et al., 2013;Hoffman and Schrag, 2002).

For the Doushantuo Fm, $\delta^{18}O$ and $\delta^{13}C$ values range from -12.15 to -6.93 ‰ and -6.24 to -3.25 ‰, respectively (Table 3). A similar range was previously reported by Jiang et al. (2003) and Zhou et al. (2004) at other locations (excluding the exotic C isotopic compositions

Clim. Past Discuss., https://doi.org/10.5194/cp-2018-119
Manuscript under review for journal Clim. Past
Discussion started: 20 September 2018

of clotted microcrystalline limestones and peloids in Jiang et al. (2003)). Both Nuccaleena and Doushantuo Fms show upward decreasing $\delta^{13}C$ values (Figure 3), in agreement with previous observations on Marinoan cap carbonates (e.g. Zhou et al. (2004)). This has been proposed to reflect a massive alkalinity flux to the oceans resulting from rapid post-glaciation weathering (Hoffman et al., 1998). This hypothesis has been challenged by a lack of significant variation in $^{87}Sr/^{86}Sr$ throughout the cap carbonate sequence (Kennedy et al., 2001), although recent studies have shown that a post-glacial meltwater is consistent with Sr isotopes or rare earth element compositions (Verdel et al., 2018;Liu et al., 2014). Oxygen and C isotope compositions correlate positively (Figure 4), also consistent with previous studies and interpreted as diagenetic overprint of primary compositions (e.g. Jiang et al. (2003)).

Lithium isotopic composition (expressed as $\delta^{7}Li$) in leaching solutions range from 2.9 to 13.7 ‰ in the Nuccaleena Fm (Table 2) and from 3.0 to 13.0 ‰ in the Doushantuo Fm (Table 3). This range is at the lower end of values encountered in Phanerozoic carbonates (Pogge von Strandmann et al., 2017a;Pogge von Strandmann et al., 2013;Lechler et al., 2015;Sun et al., 2018;Misra and Froelich, 2012). While ranges of values are similar in both sections, the Doushantuo Fm shows values systematically lower than those of the Nuccaleena (Figure 5).

5. Discussion

5.1. Dolomitisation and diagenesis

Several mechanisms have been proposed for cap dolostone formation: early, late, deep burial dolomitisation, or direct precipitation (Fairchild and Kennedy, 2007). Based on Mg and Sr isotope records in the Nuccaleena Fm also sampled at Elatina Creek, and in Mongolian cap dolostones, Liu et al. (2014) have argued that direct precipitation or early dolomitisation are the most likely scenarios. The Li isotope composition of dolostones could thus reflect that of

Clim. Past Discuss., https://doi.org/10.5194/cp-2018-119
Manuscript under review for journal Clim. Past
Discussion started: 20 September 2018

the seawater at the time of formation. This is supported by Kunzmann et al. (2013) who suggested that the Nuccaleena Fm faithfully preserves post-glacial seawater composition based on carbon and oxygen isotopic compositions. They indicated that while most dolomitized carbonates are commonly coarsely recrystallised and preferentially occur at the top of shoaling sequences, the Nuccaleena and other equivalent cap dolostones are characteristically fine-grained and were deposited at the base of a transgressive-regressive sequence (Hoffman et al., 2007). Rose and Maloof (2010) also showed consistent carbon isotopic compositions at the 1km to 100km scale in the Adelaide Rift Complex, arguing against a diagenetic overprint. Conversely, Jiang et al. (2003) suggested that the positive relationship between O and C isotope compositions in the Doushantuo Fm could reflect a diagenetic overprint of primary compositions. Huang et al. (2016) have suggested that the cap dolostone from core 14ZKZ has experienced little diagenetic alteration since it is composed of dolomicrite and microcrystalline dolostone without significant recrystallization.

To further assess the impact of diagenesis on the sections sampled, we measured oxygen and carbon isotopic compositions on bulk rock samples of both Nuccaleena and Doushantuo Fms. Measured compositions show a positive relationship between $\delta^{18}O$ and $\delta^{13}C$ for the Doushantuo Fm but not for the Nuccaleena (Figure 4), suggesting that while the former might have been affected by diagenesis, the latter may have not, in agreement with previous studies. Lighter $\delta^{7}Li$ values in Doushantuo cap dolostones compared to the Nuccaleena Fm (Figure 5), could thus be the result of a partial diagenetic overprint, or local Li isotope signal due to variable proportions of seawater-freshwater mixing between these two sites.

The effect of diagenesis on Li isotopes was also tested by comparing $\delta^{7}Li$ values to Mn/Sr ratios in the leaching solutions. The Mn/Sr ratio is often used an index for diagenetic alteration (Brand and Veizer, 1980), since diagenesis can result in a carbonate uptake of Mn. There is no clear relationship between $\delta^{7}Li$ compositions and Mn/Sr ratios for either formation

Clim. Past Discuss., https://doi.org/10.5194/cp-2018-119
Manuscript under review for journal Clim. Past
Discussion started: 20 September 2018

(Figure 6), suggesting that while diagenesis may have imparted the observed range in Mn/Sr values (in particular for the Nuccaleena Fm, which shows relatively high values), it did not have a measureable nor systematic effect on Li isotope compositions. Liu et al. (2013) observed a negative relationship between $^{87}Sr/^{86}Sr$ ratios and $\delta^{18}O$ values for Nuccaleena cap dolostones, arguing that diagenetic fluids introduced radiogenic ^{87}Sr and light oxygen isotopes. Here, there is no relationship between $\delta^{7}Li$ and $\delta^{18}O$ in either section (Figure 7), suggesting that if diagenesis resulted in an enrichment in ^{16}O, there was no associated systematic modification of the Li isotope ratio.

5.2. Lithium isotopes in Ediacaran cap carbonates and the evolution of the Neoproterozoic oceans

In the Nuccaleena Fm, $\delta^{7}Li$ values range from 7.3 to 13.7 ‰ (excluding transition zones), which contrasts with the lower values encountered in the transition zone between the Elatina and Nuccaleena Fms (<5 ‰). While Li isotope compositions were measured in leaching solutions and should be devoid of silicic-bound Li (Taylor et al., 2018), it is possible that low $\delta^{7}Li$ values in solutions of the Elatina-Nuccaleena transition zone reflect the contribution of isotopically light Li from the silicic fraction, more abundance in this part of the section (Figure 2). Interestingly, while the Nuccaleena-Brachina transition zone is also characterised by a higher silicic content (Figure 2), measured $\delta^{7}Li$ compositions in leaching solutions (6.2-11.7 ‰) are similar to those of the Nuccaleena Fm. Consequently, it is possible that the low $\delta^{7}Li$ values in the Elatina-Nuccaleena transition zone faithfully reflect the composition of the carbonate fraction, and thus of the ocean at the time. In Lower Dolomite Member of the Doushantuo Fm, $\delta^{7}Li$ compositions are overall lower than those in the Nuccaleena Fm by ~2 ‰ (calculated by comparing averages for each formation, excluding $\delta^{7}Li$ values in transition

Clim. Past Discuss., https://doi.org/10.5194/cp-2018-119
Manuscript under review for journal Clim. Past
Discussion started: 20 September 2018

zones for the Nuccaleena Fm). As indicated above, this offset could possibly be the result of diagenetic alteration of the Doushantuo Fm.

Lithium isotope compositions of the cap dolostones show little variations throughout each section (excluding transition zones), probably indicative the Li oceanic budget did not experience any major changes during cap dolostone deposition. This is discussed further below. Values are at the lower end of the range of δ^7Li values observed for other carbonates (Pogge von Strandmann et al., 2017a;Pogge von Strandmann et al., 2013;Lechler et al., 2015;Pogge von Strandmann et al., 2017b;Misra and Froelich, 2012). However, such comparison has little value since previous studies have focused on calcium carbonates, and the extent of isotopic fractionation between solution and carbonates is different whether considering calcium or Ca-Mg carbonates (Marriott et al., 2004a;Marriott et al., 2004b;Taylor et al., 2018). The abundance of dolomite in the geological records, compared to its paucity in modern environments and the difficulty to produce it experimentally at low temperature, led to coining the term 'dolomite problem' (e.g. McKenzie, 1991;Purser et al., 1994). Microbial mediation has been proposed as a key mechanism for dolomite formation in natural environments (Vasconcelos et al., 1995;Wright, 1999;Wacey et al., 2007;Burns et al., 2000), although Arvidson and Mackenzie (1999) have shown that changes in seawater temperature and chemistry could account for the abundance of dolomite in the geological record. While the precipitation experiments in Taylor et al. (2018) were performed in absence of microbial mediation, they offer an estimate of the Li isotopic fractionation between solution and Ca-Mg carbonate, $\alpha_{prec-sol}$:

$$10^3 ln\alpha_{prec-sol} = -\frac{(2.56 \pm 0.27)\times 10^6}{T^2} + (5.8 \pm 1.3) \quad (1)$$

where T is the temperature of precipitation (in K).

The relationship above allows us to use the Li isotope composition of cap dolostones to estimate the Li isotope composition of Ediacaran seawater (and/or of the seawater-freshwater mixture), assuming the temperature of seawater during cap dolostone formation.

Clim. Past Discuss., https://doi.org/10.5194/cp-2018-119
Manuscript under review for journal Clim. Past
Discussion started: 20 September 2018

318 Knauth (2005) suggested that seawater temperature dropped by 10-15 °C between 685 and 550
319 Ma to reach Phanerozoic values (10-20 °C). Considering a seawater temperature of 10 or 40
320 °C would yield isotopic fractionation factors within error of each other (α = 0.974 ± 0.241 or
321 0.980 ± 0.243, respectively). The δ^7Li composition of seawater was calculated for temperatures
322 of cap dolostone formation of 10, 25 and 40 °C (Tables 2 & 3). In the Nuccaleena Fm, average
323 calculated seawater δ^7Li values range from 30.3 (with a seawater temperature at 40 °C) to 36.2
324 ‰ (at 10 °C) (Figure 8). These values are similar to the modern seawater composition (31.1 ±
325 0.2 ‰; (Jeffcoate et al., 2004)). This observation suggests that following deglaciation, the
326 chemistry of Ediacaran oceans evolved rapidly towards that of modern oceans (at least from
327 the standpoint of the Li cycle), since even the base of the cap dolostones suggest modern-like
328 seawater δ^7Li compositions. The Elatina-Nuccaleena transition zone shows isotopic
329 compositions that are much lighter (average values ranging from 23.9 to 29.8 ‰, depending
330 on the seawater temperature considered). As discussed above, this could indeed reflect
331 isotopically lighter compositions for the seawater at that time, illustrating the recovery in the
332 aftermath of the Marinoan glaciation, or result from an incomplete isolation of the carbonate-
333 bound Li during sample preparation.

334 Calculated seawater δ^7Li compositions are investigated further using a box model for
335 the oceanic Li cycle similar to that described in previous studies (Pogge von Strandmann et al.,
336 2013;Lechler et al., 2015). The seawater Li budget is written as follows:

337 $$\frac{dN_{Li}}{dt} = F_r + F_h - F_{sed} \quad (2)$$

338 where N_{Li} represents the mass of Li in seawater (in Gmol), F_r and F_h are the input fluxes of
339 riverine and hydrothermal Li, respectively (in Gmol/yr). F_{sed} is the output flux of Li, lumping
340 together uptake into marine sediments and alteration of oceanic crust. F_{sed} is taken to scale to
341 N_{Li} via a constant partition coefficient k (Lechler et al., 2015): $F_{sed} = k \times N_{Li}$.

342 The evolution of the seawater Li isotope ratio is written as follows:

Clim. Past Discuss., https://doi.org/10.5194/cp-2018-119
Manuscript under review for journal Clim. Past
Discussion started: 20 September 2018

$$N_{Li}\frac{dR_{SW}}{dt} = F_r(R_r - R_{SW}) + F_h(R_h - R_{SW}) - F_{sed}(R_{sed} - R_{SW}) \quad (3)$$

where R_{SW}, R_r *and* R_h are the δ^7Li compositions of seawater, the riverine and hydrothermal inputs, respectively. R_{sed} is derived from R_{SW} and assuming a constant isotopic fractionation between marine sediments and seawater of 16 ‰ (Huh et al., 1998;Misra and Froelich, 2012).

Our model does not consider an output flux of Li via subduction, similarly to Pogge von Strandmann et al. (2013);Lechler et al. (2015). The model starts at the onset of the Marinoan glaciation and the ocean is assumed to have an initial mass of Li similar to that of the modern ocean: $3.6x10^7$ Gmol (Misra and Froelich, 2012), for lack of a better constraint. In the same way, we assume modern values for the hydrothermal flux of Li and its isotopic composition: 13 Gmol/yr and 8.3 ‰, respectively (Misra and Froelich, 2012). These values are kept constant throughout the Marinoan glaciation and Ediacaran cap carbonate deposition. If the hydrothermal flux was greater than the modern value (Gernon et al., 2016), riverine Li fluxes would be required to be greater than the ones calculated below. The duration of the Marinoan glaciation is taken to be 15 Myr (Hoffman et al., 2017). The seawater δ^7Li compositions used in the model are those calculated for a temperature of 25 °C for cap dolostone formation, since we show above that the temperature does not affect greatly calculated seawater compositions. The duration of cap dolostone deposition is taken to be 3 Myr (Condon et al., 2005). A much shorter duration has been proposed (e.g. Creveling and Mitrovica, 2014;Higgins and Schrag, 2003) and model results for various durations are discussed below. However, a duration of 3 Myr is considered in most scenarios below as it leads to the most conservative estimates of riverine Li fluxes and isotopic compositions.

We first tested the effect on the model's results of a delay between the end of the Marinoan glaciation and the onset of cap carbonate deposition, as Huang et al. (2016) have suggested there is a pulse of continental weathering ~1 Myr prior to the onset of deposition of the Doushantuo Fm. We modeled two cases: one where the hydrological cycle resumed at the

Clim. Past Discuss., https://doi.org/10.5194/cp-2018-119
Manuscript under review for journal Clim. Past
Discussion started: 20 September 2018

onset of cap carbonate formation (scenario 1; Table 4 & Figure 9a), and another one where it preceded cap carbonate formation by ~1 Myr (scenario 2; Table 4 & Figure 9b). In the first case, a short pulse (0.1 Myr) of intense weathering is required, where the riverine Li flux would have been 50 times the modern value, and the riverine δ^7Li would be 35 ‰. This large riverine flux is dictated by the need to increase from seawater δ^7Li values as low as ~25 ‰ at the end of the Marinoan glaciation, to 30-35 ‰ at the base of the cap dolostone. Following this stage, the riverine Li flux would still need to be 5 times the modern value, with a riverine δ^7Li similar to the modern average river, for the remainder of cap dolostone deposition. In the second case, the million year-long stage preceding cap dolostone deposition would be characterised by a riverine Li flux three times the modern value and a high riverine δ^7Li (30 ‰). During cap dolostone deposition, the riverine Li flux and isotope composition could have been similar to modern values.

In most scenarios, we assumed that the riverine input of Li shut down during glaciation. This results in a marine Li budget at the end of the glaciation about 1/3 of that at the start. If we consider there was a delay between the end of deglaciation and the onset of cap dolostone deposition, this assumption has little impact on the model results. Even if we assumed that the riverine Li flux during glaciation was as high as 80% of the modern value, resulting in a much higher seawater δ^7Li at the end of the glaciation (~30 ‰), the model can fit the data with the same parameters (scenario 3; Table 4 & Figure 10b) as when considering a complete hydrological shutdown (scenario 2). However, if considering no delay between the end of glaciation and the onset of cap dolostone deposition, a riverine Li flux during glaciation 80% that of the modern value only requires the riverine Li flux to be 10 times the modern value during the pulse of riverine Li supply at the onset of cap dolostone deposition (scenario 4; Table 4 & Figure 10a).

Clim. Past Discuss., https://doi.org/10.5194/cp-2018-119
Manuscript under review for journal Clim. Past
Discussion started: 20 September 2018

As mentioned above, several authors have suggested that cap carbonate deposition occurred over a period of a few 100,000 years or less (e.g. Creveling and Mitrovica, 2014;Higgins and Schrag, 2003). If we consider a duration of 300,000 yr for cap carbonate deposition (scenario 5; Table 4 & Figure 12), the model parameters are very similar to those obtained with a 3 Myr duration (scenario 2). The only notable differences are that the riverine Li flux during cap carbonate deposition would be twice the modern value, and its isotopic composition would high (35 ‰). Thus, uncertainty on the duration of cap carbonate deposition does not significantly affect the model results.

The model above assumes a well-mixed ocean throughout glaciation, deglaciation and cap carbonate deposition. An alternative scenario has been invoked to explain strontium and magnesium isotope compositions of the Nuccaleena Fm where the Ediacaran ocean would have experienced stratification as a consequence of glacial meltwater pulses (Liu et al., 2013;Liu et al., 2014;Shields, 2005). We have considered such a scenario: in this case, the ocean is well mixed during stage 1 (Marinoan glaciation); however, during stage 2 (time lag between deglaciation and onset of cap carbonate deposition), the shallow ocean only receives riverine Li (meltwater plume), while the deep ocean only receives hydrothermal Li and is the only compartment that loses Li to authigenic sediments and oceanic crust alteration. During stage 3 (cap carbonate deposition), shallow and deep oceans are assumed to mixed instantaneously and then experience input and loss of Li as a well-mixed ocean for the remainder of the stage duration. More complex scenarios of stratification and overturn could be considered, however there is no data justifying such hypothesis. In the model, we consider that when the ocean is stratified, the shallow ocean represents 20% of the total oceanic volume (scenario 6; Table 4 & Figure 12). Values ranging between 10 and 50% yield identical results (not shown). This lack of sensitivity to the size of the shallow and deep compartments mainly stems from the short duration of isolation. Model results are very similar to the well-mixed ocean scenario

Clim. Past Discuss., https://doi.org/10.5194/cp-2018-119
Manuscript under review for journal Clim. Past
Discussion started: 20 September 2018

(scenario 2), the only notable difference being that the stratified ocean scenario requires a riverine Li flux during cap carbonate deposition five times greater than the modern value.

Overall, the model suggests a pulse of riverine Li that lasted 0.1 to 1 Myr, and was three to 50 times greater than the modern flux. In all scenarios, the Li isotopic composition of the average riverine input during this stage was ~30-35 ‰. This value is comparable to the composition of modern Icelandic rivers (Pogge von Strandmann et al., 2006;Vigier et al., 2009). During cap carbonate deposition, most scenarios suggest that the pulse in riverine Li was followed by a flux comparable to the modern value, and with an isotopic composition also comparable to that of the average modern river, yielding Li isotope compositions for the Ediacaran ocean similar to those observed since the Pliocene.

In the aftermath of the Marinoan glaciation, new rivers would thus have drained landscapes similar to modern high latitude regions. This type of environment would have dominated exposed continents for up to 1 Myr. After that, Ediacaran landmasses could have already experienced climatic and environmental conditions similar to those experienced in the late Cenozoic. This model suggests that Ediacaran oceans and continents rapidly recovered from the deglaciation, and within a million year of the end of the Marinoan glaciation, Earth's surface was possibly resembling our modern environment. The large flux of riverine Li during deglaciation would have been accompanied by a large supply of other nutrients. If this nutrient pulse lasted one million years (scenarios 2, 3, 5 & 6), it could have been the key for the development of complex lifeforms since substantial "bursts" in evolution require million-year long changes (Uyeda et al., 2011).

6. Conclusions

The lithium isotope composition of cap dolostones of the Nuccaleena (Australia) and Doushantuo (China) Fms provide insights into the environmental changes which occurred in

the aftermath of the Marinoan glaciation. Several lines of evidence argue for a primary origin for the dolomite of these cap carbonates, which are thus believed to inform on the chemistry of the Ediacaran oceans. The Nuccaleena Fm shows no significant signs of diagenetic alteration and its Li isotope composition is likely to reflect isotopic fractionation during cap carbonate deposition. It is less clear for the Doushantuo Fm, and the ~2 ‰ offset in δ^7Li values compared to the Nuccaleena Fm could possibly be the result of partial overprinting by diagenetic fluids.

The estimated Li isotope composition of Ediacaran seawater was used in combination with an ocean box model to investigate changes in the oceanic Li cycle. Most scenarios suggest a pulse of riverine Li flux up to 50 times the modern value, during the deglaciation, with a riverine δ^7Li similar to that of rivers in modern high latitude regions. This episode lasted up to 1 Myr, after which the supply of riverine Li would have been similar to what oceans have experienced since the Pliocene. These results suggest that Ediacaran oceans and continents rapidly recovered from the Marinoan glaciation, and within 1 Myr of the onset of deglaciation the planet returned to a greenhouse state. The million-year pulse of continent-derived nutrients could have promoted the emergence of complex lifeforms, which would have thrived in an Earth surface system possibly not that different from that of the late Cenozoic.

Author contribution

AD and JF designed the project. AD, HLT, JF, AJC conducted fieldwork in Australia, BS provided Chinese samples. HLT conducted the element concentration and lithium isotope analyses. AK conducted oxygen and carbon isotope analyses. AD, JF, GMC and BS interpreted the results. AD conducted the numerical modelling and wrote the manuscript. All authors edited the manuscript.

Acknowledgments

Clim. Past Discuss., https://doi.org/10.5194/cp-2018-119
Manuscript under review for journal Clim. Past
Discussion started: 20 September 2018

467 We would like to thank Lili Yu and Leo Rothacker for help in collecting the Li isotopic
468 data, and Magali Roux for help in the field and comments on the manuscript. HT acknowledges
469 an Australian Postgraduate Award. We also thank Arthur Coulthard, the Ikara-Flinders Ranges
470 National Park and the Department of Environment, Water and Natural Resources (DEWNR)
471 for granting us permission to collect samples from Elatina Creek (research permit Y26506-2).
472 Fieldwork for this work was funded by a GeoQuEST grant to AD. Stable isotope analyses were
473 supported by the NIWA core funded project “Climate Present and Past”.

References

Arvidson, R. S., and Mackenzie, F. T.: The dolomite problem; control of precipitation kinetics by temperature and saturation state, American Journal of Science, 299, 257-288, 1999.

Balter, V., and Vigier, N.: Natural variations of lithium isotopes in a mammalian model, Metallomics, 6, 582-586, 10.1039/C3MT00295K, 2014.

Bao, H., Lyons, J. R., and Zhou, C.: Triple oxygen isotope evidence for elevated CO2 levels after a Neoproterozoic glaciation, Nature, 453, 504-506, 10.1038/nature06959, 2008.

Brand, U., and Veizer, J.: Chemical diagenesis of a multicomponent carbonate system--1: Trace elements, Journal of Sedimentary Research, 50, 1980.

Brocks, J. J., Jarrett, A. J. M., Sirantoine, E., Hallmann, C., Hoshino, Y., and Liyanage, T.: The rise of algae in Cryogenian oceans and the emergence of animals, Nature, 548, 578-581, 10.1038/nature23457, 2017.

Burns, S. J., Mckenzie, J. A., and Vasconcelos, C.: Dolomite formation and biogeochemical cycles in the Phanerozoic, Sedimentology, 47, 49-61, 2000.

Burton, K. W., and Vigier, N.: Lithium Isotopes as Tracers in Marine and Terrestrial Environments, in: Handbook of Environmental Isotope Geochemistry, edited by: Baskaran, M., Advances in Isotope Geochemistry, Springer Berlin Heidelberg, 41-59, 2011.

Carignan, J., Vigier, N., and Millot, R.: Three Secondary Reference Materials for Lithium Isotope Measurements: Li7 - N, Li6 - N and LiCl - N Solutions, Geostandards and Geoanalytical Research, 31, 7-12, 2007.

Chen, D. F., Dong, W. Q., Zhu, B. Q., and Chen, X. P.: Pb–Pb ages of Neoproterozoic Doushantuo phosphorites in South China: constraints on early metazoan evolution and glaciation events, Precambrian Res, 132, 123-132, https://doi.org/10.1016/j.precamres.2004.02.005, 2004.

Condon, D., Zhu, M., Bowring, S., Wang, W., Yang, A., and Jin, Y.: U-Pb ages from the neoproterozoic Doushantuo Formation, China, Science, 308, 95-98, 2005.

Creveling, J. R., and Mitrovica, J. X.: The sea-level fingerprint of a Snowball Earth deglaciation, Earth and Planetary Science Letters, 399, 74-85, 2014.

Decarreau, A., Vigier, N., Pálková, H., Petit, S., Vieillard, P., and Fontaine, C.: Partitioning of lithium between smectite and solution: An experimental approach, Geochimica et Cosmochimica Acta, 85, 314-325, 2012.

Fairchild, I. J., and Kennedy, M. J.: Neoproterozoic glaciation in the Earth System, Journal of the Geological Society, 164, 895-921, 2007.

Flesch, G., Anderson, A., and Svec, H.: A secondary isotopic standard for 6Li/7Li determinations, International Journal of Mass Spectrometry and Ion Physics, 12, 265-272, 1973.

Font, E., Nédélec, A., Trindade, R., and Moreau, C.: Fast or slow melting of the Marinoan snowball Earth? The cap dolostone record, Palaeogeography, Palaeoclimatology, Palaeoecology, 295, 215-225, 2010.

Gernon, T. M., Hincks, T. K., Tyrrell, T., Rohling, E. J., and Palmer, M. R.: Snowball Earth ocean chemistry driven by extensive ridge volcanism during Rodinia breakup, Nature Geoscience, 9, 242-248, 10.1038/ngeo2632, 2016.

Higgins, J. A., and Schrag, D. P.: Aftermath of a snowball Earth, Geochemistry, Geophysics, Geosystems, 4, 2003.

Hoffman, P. F., Kaufman, A. J., Halverson, G. P., and Schrag, D. P.: A Neoproterozoic snowball earth, Science, 281, 1342-1346, 1998.

Hoffman, P. F., and Schrag, D. P.: The snowball Earth hypothesis: testing the limits of global change, Terra nova, 14, 129-155, 2002.

Hoffman, P. F., Halverson, G. P., Domack, E. W., Husson, J. M., Higgins, J. A., and Schrag, D. P.: Are basal Ediacaran (635 Ma) post-glacial "cap dolostones" diachronous?, Earth and Planetary Science Letters, 258, 114-131, 2007.

Hoffman, P. F., Abbot, D. S., Ashkenazy, Y., Benn, D. I., Brocks, J. J., Cohen, P. A., Cox, G. M., Creveling, J. R., Donnadieu, Y., Erwin, D. H., Fairchild, I. J., Ferreira, D., Goodman, J. C., Halverson, G. P., Jansen, M. F., Le Hir, G., Love, G. D., Macdonald, F. A., Maloof, A. C., Partin, C. A., Ramstein, G., Rose, B. E. J., Rose, C. V., Sadler, P. M., Tziperman, E., Voigt, A., and Warren, S. G.: Snowball Earth climate dynamics and Cryogenian geology-geobiology, Science Advances, 3, 10.1126/sciadv.1600983, 2017.

Huang, K.-J., Teng, F.-Z., Shen, B., Xiao, S., Lang, X., Ma, H.-R., Fu, Y., and Peng, Y.: Episode of intense chemical weathering during the termination of the 635 Ma Marinoan glaciation, Proceedings of the National Academy of Sciences, 10.1073/pnas.1607712113, 2016.

Huh, Y., Chan, L. H., Zhang, L., and Edmond, J. M.: Lithium and its isotopes in major world rivers: implications for weathering and the oceanic budget, Geochimica et Cosmochimica Acta, 62, 2039-2051, 1998.

Hyde, W. T., Crowley, T. J., Baum, S. K., and Peltier, W. R.: Neoproterozoic 'snowball Earth'simulations with a coupled climate/ice-sheet model, Nature, 405, 425, 2000.

Jeffcoate, A. B., Elliott, T., Thomas, A., and Bouman, C.: Precise/ Small Sample Size Determinations of Lithium Isotopic Compositions of Geological Reference Materials and Modern Seawater by MC-ICP-MS, Geostandards and Geoanalytical Research, 28, 161-172, 10.1111/j.1751-908X.2004.tb01053.x, 2004.

Jenkins, R.: The Adelaide fold belt: tectonic reappraisal, The evolution of a Late Precambrian–Early Palaeozoic Rift Complex: The Adelaide Geosyncline, 16, 395-420, 1990.

Jiang, G., Kennedy, M. J., and Christie-Blick, N.: Stable isotopic evidence for methane seeps in Neoproterozoic postglacial cap carbonates, Nature, 426, 822, 2003.

Jiang, G., Shi, X., Zhang, S., Wang, Y., and Xiao, S.: Stratigraphy and paleogeography of the Ediacaran Doushantuo Formation (ca. 635–551 Ma) in south China, Gondwana Research, 19, 831-849, 2011.

John, S. G., Kunzmann, M., Townsend, E. J., and Rosenberg, A. D.: Zinc and cadmium stable isotopes in the geological record: A case study from the post-snowball Earth Nuccaleena cap dolostone, Palaeogeography, Palaeoclimatology, Palaeoecology, 466, 202-208, 10.1016/j.palaeo.2016.11.003, 2017.

Kasemann, S. A., Hawkesworth, C. J., Prave, A. R., Fallick, A. E., and Pearson, P. N.: Boron and calcium isotope composition in Neoproterozoic carbonate rocks from Namibia: Evidence for extreme environmental change, Earth and Planetary Science Letters, 231, 73-86, 2005.

Kennedy, M. J., Christie-Blick, N., and Prave, A. R.: Carbon isotopic composition of Neoproterozoic glacial carbonates as a test of paleoceanographic models for snowball Earth phenomena, Geology, 29, 1135-1138, 2001.

Knauth, L. P.: Temperature and salinity history of the Precambrian ocean: implications for the course of microbial evolution, Palaeogeography, Palaeoclimatology, Palaeoecology, 219, 53-69, https://doi.org/10.1016/j.palaeo.2004.10.014, 2005.

Knoll, A. H., and Carroll, S. B.: Early animal evolution: emerging views from comparative biology and geology, Science, 284, 2129-2137, 1999.

Kunzmann, M., Halverson, G. P., Sossi, P. A., Raub, T. D., Payne, J. L., and Kirby, J.: Zn isotope evidence for immediate resumption of primary productivity after snowball Earth, Geology, 41, 27-30, 10.1130/g33422.1, 2013.

Lechler, M., Pogge von Strandmann, P. A. E., Jenkyns, H. C., Prosser, G., and Parente, M.: Lithium-isotope evidence for enhanced silicate weathering during OAE 1a (Early Aptian Selli

event), Earth and Planetary Science Letters, 432, 210-222, http://dx.doi.org/10.1016/j.epsl.2015.09.052, 2015.
Li, G., and West, A. J.: Evolution of Cenozoic seawater lithium isotopes: Coupling of global denudation regime and shifting seawater sinks, Earth and Planetary Science Letters, 401, 284-293, http://dx.doi.org/10.1016/j.epsl.2014.06.011, 2014.
Liu, C., Wang, Z., and Raub, T. D.: Geochemical constraints on the origin of Marinoan cap dolostones from Nuccaleena Formation, South Australia, Chemical Geology, 351, 95-104, https://doi.org/10.1016/j.chemgeo.2013.05.012, 2013.
Liu, C., Wang, Z., Raub, T. D., Macdonald, F. A., and Evans, D. A. D.: Neoproterozoic cap-dolostone deposition in stratified glacial meltwater plume, Earth and Planetary Science Letters, 404, 22-32, 10.1016/j.epsl.2014.06.039, 2014.
Love, G. D., Grosjean, E., Stalvies, C., Fike, D. A., Grotzinger, J. P., Bradley, A. S., Kelly, A. E., Bhatia, M., Meredith, W., Snape, C. E., Bowring, S. A., Condon, D. J., and Summons, R. E.: Fossil steroids record the appearance of Demospongiae during the Cryogenian period, Nature, 457, 718-721, http://www.nature.com/nature/journal/v457/n7230/suppinfo/nature07673_S1.html, 2009.
Maloof, A. C., Rose, C. V., Beach, R., Samuels, B. M., Calmet, C. C., Erwin, D. H., Poirier, G. R., Yao, N., and Simons, F. J.: Possible animal-body fossils in pre-Marinoan limestones from South Australia, Nature Geoscience, 3, 653-659, 10.1038/ngeo934, 2010.
Marriott, C. S., Henderson, G. M., Belshaw, N. S., and Tudhope, A. W.: Temperature dependence of δ 7 Li, δ 44 Ca and Li/Ca during growth of calcium carbonate, Earth and Planetary Science Letters, 222, 615-624, 2004a.
Marriott, C. S., Henderson, G. M., Crompton, R., Staubwasser, M., and Shaw, S.: Effect of mineralogy, salinity, and temperature on Li/Ca and Li isotope composition of calcium carbonate, Chemical Geology, 212, 5-15, 2004b.
Millot, R., Vigier, N., and Gaillardet, J.: Behaviour of lithium and its isotopes during weathering in the Mackenzie Basin, Canada, Geochimica et Cosmochimica Acta, 74, 3897-3912, 10.1016/j.gca.2010.04.025, 2010.
Misra, S., and Froelich, P. N.: Lithium isotope history of Cenozoic seawater: Changes in silicate weathering and reverse weathering, Science, 335, 818-823, DOI 10.1126/science.1214697, 2012.
Och, L. M., and Shields-Zhou, G. A.: The Neoproterozoic oxygenation event: Environmental perturbations and biogeochemical cycling, Earth-Science Reviews, 110, 26-57, 2012.
Ohnemueller, F., Prave, A. R., Fallick, A. E., and Kasemann, S. A.: Ocean acidification in the aftermath of the Marinoan glaciation, Geology, 42, 1103-1106, 2014.
Pistiner, J. S., and Henderson, G. M.: Lithium-isotope fractionation during continental weathering processes, Earth and Planetary Science Letters, 214, 327-339, 10.1016/s0012-821x(03)00348-0, 2003.
Pogge von Strandmann, P. A. E., Burton, K. W., James, R. H., Van Calsteren, P., Gislason, S. R., and Mokadem, F.: Riverine behaviour of uranium and lithium isotopes in an actively glaciated basaltic terrain, Earth and Planetary Science Letters, 251, 134-147, 2006.
Pogge von Strandmann, P. A. E., Jenkyns, H. C., and Woodfine, R. G.: Lithium isotope evidence for enhanced weathering during Oceanic Anoxic Event 2, Nature Geosci, 6, 668-672, 10.1038/ngeo1875
http://www.nature.com/ngeo/journal/v6/n8/abs/ngeo1875.html#supplementary-information, 2013.
Pogge von Strandmann, P. A. E., Desrochers, A., Murphy, M. J., Finlay, A. J., Selby, D., and Lenton, T. M.: Global climate stabilisation by chemical weathering during the Hirnantian glaciation, Geochemical Perspectives Letters, 230-237, 10.7185/geochemlet.1726, 2017a.

620 Pogge von Strandmann, P. A. E., Vaks, A., Bar-Matthews, M., Ayalon, A., Jacob, E., and
621 Henderson, G. M.: Lithium isotopes in speleothems: Temperature-controlled variation in
622 silicate weathering during glacial cycles, Earth and Planetary Science Letters, 469, 64-74,
623 https://doi.org/10.1016/j.epsl.2017.04.014, 2017b.
624 Preiss, W. V.: The Adelaide Geosyncline: Late Proterozoic stratigraphy, sedimentation,
625 palaeontology and tectonics, 53, Department of Mines and Energy, 1987.
626 Purser, B., Tucker, M., and Zenger, D.: Problems, progress and future research concerning
627 dolomites and dolomitization, Dolomites: A volume in honour of Dolomieu, 1-20, 1994.
628 R Core Team: R: A language and environment for statistical computing, R Foundation for
629 Statistical Computing, Vienna, Australia, 2013.
630 Raub, T. D., Evans, D. A. D., and Smirnov, A. V.: Siliciclastic prelude to Elatina–Nuccaleena
631 deglaciation: lithostratigraphy and rock magnetism of the base of the Ediacaran system,
632 Geological Society, London, Special Publications, 286, 53-76, 10.1144/sp286.5, 2007.
633 Raub, T. D.: Prolonged Deglaciation of "Snowball Earth", Ph.D., Yale University, 299 pp.,
634 2008.
635 Rose, C. V., and Maloof, A. C.: Testing models for post-glacial 'cap dolostone' deposition:
636 Nuccaleena Formation, South Australia, Earth and Planetary Science Letters, 296, 165-180,
637 10.1016/j.epsl.2010.03.031, 2010.
638 Sahoo, S. K., Planavsky, N. J., Jiang, G., Kendall, B., Owens, J. D., Wang, X., Shi, X., Anbar,
639 A. D., and Lyons, T. W.: Oceanic oxygenation events in the anoxic Ediacaran ocean,
640 Geobiology, 10.1111/gbi.12182, 2016.
641 Scott, C., Lyons, T., Bekker, A., Shen, Y.-a., Poulton, S., Chu, X.-l., and Anbar, A.: Tracing
642 the stepwise oxygenation of the Proterozoic ocean, Nature, 452, 456, 2008.
643 Shields, G. A.: Neoproterozoic cap carbonates: a critical appraisal of existing models and the
644 plumeworld hypothesis, Terra Nova, 17, 299-310, 2005.
645 Sun, H., Xiao, Y., Gao, Y., Zhang, G., Casey, J. F., and Shen, Y.: Rapid enhancement of
646 chemical weathering recorded by extremely light seawater lithium isotopes at the Permian-
647 Triassic boundary, Proc Natl Acad Sci U S A, 115, 3782-3787, 10.1073/pnas.1711862115,
648 2018.
649 Taylor, H., Kell Duivestein, I. J., Farkas, J., Dietzel, M., and Dosseto, A.: Lithium isotopes in
650 dolostone as a palaeo-environmental proxy – An experimental approach, Earth Surface
651 Dynamics, pre-print, 2018.
652 Uyeda, J. C., Hansen, T. F., Arnold, S. J., and Pienaar, J.: The million-year wait for
653 macroevolutionary bursts, Proc Natl Acad Sci U S A, 108, 15908-15913,
654 10.1073/pnas.1014503108, 2011.
655 Vasconcelos, C., McKenzie, J. A., Bernasconi, S., Grujic, D., and Tiens, A. J.: Microbial
656 mediation as a possible mechanism for natural dolomite formation at low temperatures, Nature,
657 377, 220, 10.1038/377220a0, 1995.
658 Verdel, C., Phelps, B., and Welsh, K.: Rare earth element and $^{87}Sr/^{86}Sr$ step-leaching
659 geochemistry of central Australian Neoproterozoic carbonate, Precambrian Res, 310, 229-242,
660 2018.
661 Verney-Carron, A., Vigier, N., and Millot, R.: Experimental determination of the role of
662 diffusion on Li isotope fractionation during basaltic glass weathering, Geochimica et
663 Cosmochimica Acta, 75, 3452-3468, 2011.
664 Vigier, N., Gislason, S. R., Burton, K. W., Millot, R., and Mokadem, F.: The relationship
665 between riverine lithium isotope composition and silicate weathering rates in Iceland, Earth
666 and Planetary Science Letters, 287, 434-441, 10.1016/j.epsl.2009.08.026, 2009.
667 Vigier, N., and Goddéris, Y.: A new approach for modeling Cenozoic oceanic lithium isotope
668 paleo-variations: the key role of climate, Climate of the Past, 11, 635-645, 10.5194/cp-11-635-
669 2015, 2015.

Wacey, D., Wright, D. T., and Boyce, A. J.: A stable isotope study of microbial dolomite formation in the Coorong Region, South Australia, Chemical Geology, 244, 155-174, 2007.
Wanner, C., Sonnenthal, E. L., and Liu, X.-M.: Seawater δ7Li: A direct proxy for global CO2 consumption by continental silicate weathering?, Chemical Geology, http://dx.doi.org/10.1016/j.chemgeo.2014.05.005, 2014.
Wickham, H.: ggplot2: Elegant Graphics for Data Analysis, Springer-Verlag New York, 2016.
Wimpenny, J., Gíslason, S. R., James, R. H., Gannoun, A., Pogge Von Strandmann, P. A. E., and Burton, K. W.: The behaviour of Li and Mg isotopes during primary phase dissolution and secondary mineral formation in basalt, Geochimica et Cosmochimica Acta, 74, 5259-5279, 2010.
Wright, D. T.: The role of sulphate-reducing bacteria and cyanobacteria in dolomite formation in distal ephemeral lakes of the Coorong region, South Australia, Sedimentary Geology, 126, 147-157, 1999.
Yin, L., Zhu, M., Knoll, A. H., Yuan, X., Zhang, J., and Hu, J.: Doushantuo embryos preserved inside diapause egg cysts, Nature, 446, 661, 2007.
Yin, Z., Zhu, M., Davidson, E. H., Bottjer, D. J., Zhao, F., and Tafforeau, P.: Sponge grade body fossil with cellular resolution dating 60 Myr before the Cambrian, Proceedings of the National Academy of Sciences, 201414577, 2015.
Yuan, X., Chen, Z., Xiao, S., Zhou, C., and Hua, H.: An early Ediacaran assemblage of macroscopic and morphologically differentiated eukaryotes, Nature, 470, 390, 2011.
Zhou, C., Tucker, R., Xiao, S., Peng, Z., Yuan, X., and Chen, Z.: New constraints on the ages of Neoproterozoic glaciations in south China, Geology, 32, 10.1130/g20286.1, 2004.

Clim. Past Discuss., https://doi.org/10.5194/cp-2018-119
Manuscript under review for journal Clim. Past
Discussion started: 20 September 2018

Climate of the Past Discussions

694 **Figure captions**

695 Figure 1. (a) Map showing the Doushantuo Fm in the context of a simplified geological map
696 of southern China. The blow-up inset shows the location of the studied core (14ZK). Modified
697 from Huang et al. (2016). (b) Simplified geological map of the central Flinders Ranges,
698 Australia (inset: the square shows the location of the Flinders Ranges in Australia). The
699 sampling site (Elatina Creek) is indicated as a red circle. Modified from Maloof et al. (2010).
700
701 Figure 2. Dolomite (green circles), muscovite (red) and quartz (blue) concentrations in cap
702 carbonates of the Nuccaleena Formation, as a function of the height above the base of the
703 formation. The curves are polynomial fits shown with 95% confidence intervals (grey areas),
704 calculated using the function *loess* in R (R Core Team, 2013). The base and top of the
705 Nuccaleena Formation show a higher proportion of detrital minerals. Note that this is unlikely
706 to affect Li isotopic compositions, since they were measured on leaching solutions, which
707 selectively target the carbonate fraction. All figures were drafted using the *ggplot2* package in
708 R (Wickham, 2016).
709
710 Figure 3. Carbon isotopic compositions in cap dolostones, as a function of the height above the
711 base of the formation (blue: Nuccaleena, red: Doushantuo). Carbon isotopic compositions were
712 measured on bulk rock samples. External uncertainty (2σ) is smaller than the symbol size.
713
714 Figure 4. Carbon and oxygen isotopic compositions in the Nuccaleena (blue) and Doushanto
715 Formation (red) Fms. The Doushanto cap dolostones show a positive correlation between C
716 and O isotopic compositions (R^2 = 0.49; excluding the sample with a $\delta^{13}C$ > -4 ‰), suggesting
717 a possible diagenetic overprint; this is not observed in the Nuccaleena Fm. External uncertainty
718 (2σ) is smaller than the symbol size.
719
720 Figure 5. Lithium isotopic compositions in cap dolostones, as a function of the above the base
721 of the formation. Lithium isotopic compositions were measured on leaching. The curves are
722 polynomial fits shown with 95% confidence intervals (grey areas), calculated using the
723 function *loess* in R and a span value of 0.6. Errors bars show the 2σ external uncertainty.
724
725 Figure 6. Lithium isotopic compositions as a function of Mn/Sr ratios in leaching solutions of
726 Nuccaleena (blue) and Doushantuo (red) cap dolostones. Errors bars show the 2σ external
727 uncertainty.
728
729 Figure 7. Lithium isotopic compositions in leaching solutions as a function of oxygen isotopic
730 compositions of bulk samples in the Nuccaleena (blue) and Doushanto Formation (red) Fms.
731 The error bar in the top left corner shows the 2σ external uncertainty on δ^7Li values.
732
733 Figure 8. Calculated seawater Li isotopic compositions for the Nuccaleena Fm, as a function
734 of the height above the base of the formation. The composition of seawater is calculated using
735 that of cap dolostone leaching solutions, and the relationship between dolomite and temperature
736 determined experimentally in Taylor et al. (2018). Temperatures considered for dolostone
737 formation are 10 (blue symbols), 25 (green) and 40 (red) °C. Curves are polynomial fits shown
738 with 95% confidence intervals (grey areas), calculated using the function *loess* in R. The grey
739 areas show the Elatina-Nuccaleena and Nuccaleena-Brachina transition zones.
740
741 Figure 9. Modelled seawater Li isotopic compositions (black curves) and calculated seawater
742 compositions for the Nuccaleena Fm (blue), as a function of the height above the base of each

Clim. Past Discuss., https://doi.org/10.5194/cp-2018-119
Manuscript under review for journal Clim. Past
Discussion started: 20 September 2018

743 formation. Seawater compositions were calculated for a temperature of dolostone formation of
744 25 °C. (a) The hydrological cycle resumes at the onset of cap carbonate deposition (scenario 1;
745 Table 4); (b) the hydrological cycle resumes 1 Myr before the onset of cap carbonate deposition
746 (scenario 2; Table 4).
747
748 Figure 10. Modelled seawater Li isotopic compositions (black curves) and calculated seawater
749 compositions for the Nuccaleena Fm (blue), as a function of the height above the base of each
750 formation. Seawater compositions were calculated for a temperature of dolostone formation of
751 25 °C. For each model curve, during the Marinoan glaciation, the riverine Li supply to the
752 oceans is 80% that of the modern value. (a) The hydrological cycle resumes at the onset of cap
753 carbonate deposition (scenario 4; Table 4); (b) the hydrological cycle resumes 1 Myr before
754 the onset of cap carbonate deposition (scenario 3; Table 4).
755
756 Figure 11. Modelled seawater Li isotopic compositions (black curves) and calculated seawater
757 compositions for the Nuccaleena Fm (blue), as a function of the height above the base of each
758 formation. Seawater compositions were calculated for a temperature of dolostone formation of
759 25 °C. The model curve is calculated assuming a duration of cap dolostone deposition of 0.3
760 Myr (scenario 5; Table 4).
761
762 Figure 12. Modelled seawater Li isotopic compositions (black curves) and calculated seawater
763 compositions for the Nuccaleena Fm (blue), as a function of the height above the base of each
764 formation. Seawater compositions were calculated for a temperature of dolostone formation of
765 25 °C. The model curve is calculated assuming a stratified ocean during stage 2 (deglaciation)
766 while the ocean is well-mixed during stages 1 (glaciation) and 3 (cap dolostone deposition)
767 (scenario 6; Table 4).

Clim. Past Discuss., https://doi.org/10.5194/cp-2018-119
Manuscript under review for journal Clim. Past
Discussion started: 20 September 2018

Climate of the Past Discussions
Open Access
EGU

768 **Tables**

769 Table 1. Mineral concentrations in bulk rock samples of the Nuccaleena Formation at Elatina Creek

Sample ID	Height above the base of the formation (m)	Quartz	Aragonite	Albite	Calcite	Dolomite	Ankerite	Siderite	Kaolinite	Chlorite	Illite	Muscovite
EC1	-0.6	-	-	-	-	-	-	-	-	-	-	-
EC2	-0.3	32	1.1	11	0	35	0.9	0.1	2.1	2.7	0	15
EC3	-0.1	20	0	1.7	0.2	63	3.6	1.3	1.7	1.2	0	6.6
EC4	0.1	4.1	0	0	4.6	80	6.4	0.8	1.1	0	0.8	2.1
EC5	0.2	2.6	0	0	3	84	4.5	0.6	0.5	0	0	4.8
EC6	0.35	4.0	0.2	0	7.9	74	6.2	0	0.3	0	0	6.6
EC7	0.45	3.0	0.4	0	2.4	83	4.8	0.4	0.5	0	0	4.6
EC8	0.45	3.6	0.1	0	1.9	83	6.4	0	0.4	0	0.1	3.6
EC9	0.55	4.3	0.3	0	2.6	81	6.4	0.2	0.3	0	0	4.6
EC10	1.0	3.3	0.1	0	0.8	79	10	0.7	0.3	0	1.1	4.1
EC11	1.2	5.9	0.4	0.1	3.7	75	10.4	0.7	0.6	0	1.3	1.9
EC12	1.35	4.3	0.3	0	6.3	73	5	1.4	0.9	0	0	8.5
EC13	1.4	8.7	0.5	0	7.1	70	6.4	0.4	0.3	0	0.3	6.1
EC14	1.7	4.8	0.1	0	5.8	74	8.2	0.4	1.4	0	0	5.4
EC15	1.8	4.2	0	0	11	71	5.8	1.2	0.7	0	0	6.3
EC16	1.9	2.4	0.2	0	0.8	79	10.8	0.6	0.3	0	1.2	4.7
EC17	2.5	3.8	0.2	0	1.7	78	9.9	0.1	0.4	0	0.3	5.6
EC18	3.0	7.2	0.3	0.3	0.8	79	7.2	0.8	1.1	0	0.8	2.6
EC19	3.4	8.1	0	0.1	2.1	78	7.2	0.9	0.3	0	0.9	1.8
EC20	3.6	8.9	0	0.8	1.8	78	6.3	0.4	0.4	0	0.6	2.7
EC21	3.8	9.9	0.4	1.2	0.4	77	5.6	0.9	0.6	0	1.1	2.9
EC22	3.9	6.0	0	0	1.4	83	5.8	0	0.7	0	0.2	2.8
EC23	4.1	8.4	0	0.9	1.2	76	6.4	0.2	0.8	0	0	5.5
EC24	4.1	7.6	0	1	0.3	77	7.9	0	0.9	0	0	4.3

Clim. Past Discuss., https://doi.org/10.5194/cp-2018-119
Manuscript under review for journal Clim. Past
Discussion started: 20 September 2018

Climate of the Past Discussions
Open Access
EGU

EC25	4.95	8.9	0	1.5	1.2	78	5.9	0	0.3	0	1	2.2
EC26	5.3	14	0	5.1	1.1	70	2.1	0.2	1	0.2	0	6.2
EC27	5.8	16	0	3.5	17	44	2	1.3	2.5	1.9	0	12
EC28	6.15	24	1.5	7.8	0.3	33	2.6	0.9	3.1	5.7	0	21

Concentrations are given in wt %.

Clim. Past Discuss., https://doi.org/10.5194/cp-2018-119
Manuscript under review for journal Clim. Past
Discussion started: 20 September 2018

773 Table 2. Element concentrations, lithium, oxygen and carbon isotopic compositions of the Nuccaleena Formation at Elatina Creek

Sample ID	Mg (ppm)	Ca (ppm)	Al (ppm)	Ti (ppm)	Mn (ppm)	Rb (ppb)	Sr (ppb)	Li (ppb)	δ^7Li (‰)	δ^{13}C	δ^{18}O	δ^7Li_{sw} @10°C (‰)	δ^7Li_{sw} @25°C (‰)	δ^7Li_{sw} @40°C (‰)
EC1	143	125	29.4	1.45	4.23	35.8	435	141	2.9			29.0	25.9	23.2
EC2	288	214	15.2	2.77	9.15	22.7	344	44	3.1	-1.06	-6.87	29.2	26.1	23.4
EC3	303	220	15.6	2.89	9.92	14.6	330	36	4.9	-1.12	-7.51	31.0	27.9	25.2
EC4	242	280	30.8	3.8	2.63	8.1	572	27	11.6	-2	-8.02	37.7	34.6	31.9
EC5	217	296	17.3	3.82	1.91	8.5	405	19	11.2	-2.21	-7.41	37.3	34.2	31.5
EC6	191	305	16	3.98	0.47	12.9	524	28	9.7	-2.91	-6.29	35.8	32.7	30.0
EC7	233	274	25.3	3.51	1.32	6.2	346	22	8.1	-2.13	-7.68	34.2	31.1	28.4
EC8	242	268	17.1	3.37	1.82	7.7	435	22	10	-1.73	-7.89	36.1	33.0	30.3
EC9	223	277	14.7	3.56	0.98	14.2	389	25	11.9	-1.96	-7.08	38.0	34.9	32.2
EC10	330	222	16.7	2.85	0.78	11.2	285	34	7.3	-2.13	-7.85	33.4	30.3	27.6
EC11	210	273	19.8	3.52	0.59	23.7	352	39	9.4	-2.49	-7.34	35.5	32.4	29.7
EC12	130	351	19.9	4.57	1.77	8.1	364	28	11.3	-2.28	-7.65	37.4	34.3	31.6
EC13	189	292	22.7	3.78	3.7	14.9	294	23	10.3	-2.67	-6.83	36.4	33.3	30.6
EC14	138	341	21.4	4.44	2.24	8.9	333	32	10.8	-2.89	-7.73	36.9	33.8	31.1
EC15	112	355	18	4.7	0.8	9.3	343	25	13.7	-3.19	-7.28	39.8	36.7	34.0
EC16	304	239	18.7	3.14	5.41	10.2	340	38	9.3	-2.34	-8.79	35.4	32.3	29.6
EC17	264	248	17.3	3.26	5.4	8	325	43	10.6	-2.34	-8.9	36.7	33.6	30.9
EC18	299	233	26.6	2.97	5.16	7.1	273	28	9.2	-2.39	-8.49	35.3	32.2	29.5
EC19	229	263	15.9	3.53	4.42	10.7	355	27	9.7	-2.57	-8.28	35.8	32.7	30.0
replicate										-2.65	-8.33			
replicate										-2.61	-8.43			
EC20	293	218	16.5	2.93	4.59	13	262	27	9.2	-2.57	-8.37	35.3	32.2	29.5
EC21	279	223	16.7	2.86	7.24	6	287	26	9.7	-2.52	-8.72	35.8	32.7	30.0
EC22	264	235	15.4	3.08	6.51	4.5	268	21	9.4	-2.49	-8.05	35.5	32.4	29.7
EC23	284	223	20.1	2.86	2.88	15.2	296	24	10.3	-2.2	-8.48	36.4	33.3	30.6
EC24	300	216	16.7	2.8	9	18.3	245	21	8.8	-2.51	-8.29	34.9	31.8	29.1

Clim. Past Discuss., https://doi.org/10.5194/cp-2018-119
Manuscript under review for journal Clim. Past
Discussion started: 20 September 2018

EC25	269	234	25.4	3.12	2.31	8.4	603	34	11.7	-2.92	-8.06	37.8	34.7	32.0
EC26	283	218	620.4	2.89	8	12.6	310	20	9.6	-2.94	-8.23	35.7	32.6	29.9
EC27	84	343	15.6	4.56	3.13	19	331	28	7.2			33.3	30.2	27.5
EC28	269	197	15.4	2.72	11.37	22.3	340	47	6.2	-2.85	-6.92	32.3	29.2	26.5

Element concentrations and Li isotope compositions were measured in leaching solutions while oxygen and carbon isotope compositions were measured in bulk rock. External analytical uncertainty is 1.2 ‰ for $\delta^{7}Li$, 0.065 ‰ for $\delta^{13}C$ and 0.12 ‰ for $\delta^{18}O$ (2σ). $\delta^{7}Li_{sw}$ @10, 25 and 40°C are the seawater compositions calculated using the relationship between the Li isotope fractionation factor and precipitation temperature from Taylor et al. (2018), and temperatures of cap dolostone formation of 10, 25 and 40 °C.

Climate of the Past
Discussions
Open Access
EGU

Clim. Past Discuss., https://doi.org/10.5194/cp-2018-119
Manuscript under review for journal Clim. Past
Discussion started: 20 September 2018

780 Table 3. Trace element concentrations, lithium, oxygen and carbon isotopic compositions of the Doushantuo Formation in core 14ZK

Sample ID	Height above the base of the formation (m)	Mn (ppm)	Rb (ppb)	Sr (ppb)	Li (ppb)	δ^7Li (‰)	δ^7Li_{sw} @10°C (‰)	δ^7Li_{sw} @25°C (‰)	δ^7Li_{sw} @40°C (‰)	$\delta^{13}C$	$\delta^{18}O$
DST-1	0.49	8.89	32.4	2328	117	3.5	29.6	26.5	23.8	-6.24	-10.45
DST-2	0.64	0.09	<d.l.	637	63	4.1	30.2	27.1	24.4	-4.42	-9.71
replicate						5.4	31.5	28.4	25.7		
DST-3	0.7	0.81	<d.l.	1206	32	7.8	33.9	30.8	28.1	-5.55	-10.06
DST-4	0.78	0.24	<d.l.	719	37	4.2	30.3	27.2	24.5	-4.24	-9.23
DST-5	0.93	2.27	<d.l.	790	35	6.7	32.8	29.7	27.0	-4.46	-9.06
DST-6	1.08	12.29	17.9	2526	64	3	29.1	26.0	23.3	-5.28	-12.15
DST-7	1.23	6.65	<d.l.	1105	38	6.7	32.8	29.7	27.0	-5.35	-9.25
replicate						6.8	32.9	29.8	27.1		
DST-8	1.38	6.45	<d.l.	902	37	8.9	35.0	31.9	29.2	-3.25	-6.93
DST-9	1.48	0.30	<d.l.	1262	27	11.1	37.2	34.1	31.4	-4.9	-8.22
DST-10	1.63	0.42	<d.l.	1515	19	10.9	37.0	33.9	31.2	-4.81	-9.03
DST-11	1.73	0.59	1.25	1632	22	9.3	35.4	32.3	29.6	-4.93	-9.23
DST-12	1.83	7.14	1.25	1649	43	6.9	33.0	29.9	27.2		
DST-13	1.98	0.48	23.3	1932	78	5	31.1	28.0	25.3		
DST-14	2.08	0.14	<d.l.	1679	22	8	34.1	31.0	28.3	-5.03	-10.32
DST-15	2.33	0.23	0.28	1972	23	7	33.1	30.0	27.3	-4.99	-10.37
DST-16	2.63	1.82	<d.l.	1025	62	7.1	33.2	30.1	27.4	-4.63	-9.19
DST-17	2.83	1.01	<d.l.	1531	26	6.5	32.6	29.5	26.8	-4.89	-9.82
DST-18	2.98	0.16	3.74	2448	21	13	39.1	36.0	33.3	-5.08	-10.32
DST-19	3.21	2.60	1.80	1141	39	9.4	35.5	32.4	29.7	-5.41	-9.53
DST-20	3.36	2.82	0.28	827	38	10.5	36.6	33.5	30.8	-5.35	-8.72
replicate						8.8	34.9	31.8	29.1		
DST-21	3.51	3.06	<d.l.	726	33	6.7	32.8	29.7	27.0	-4.79	-8.36
DST-22	3.66	2.88	0.14	868	29	6.6	32.7	29.6	26.9	-4.83	-9.4
DST-23	3.86	0.33	<d.l.	1665	34	7.5	33.6	30.5	27.8	-5.5	-10.43

Clim. Past Discuss., https://doi.org/10.5194/cp-2018-119
Manuscript under review for journal Clim. Past
Discussion started: 20 September 2018

Climate of the Past Discussions
Open Access
EGU

DST-24	4.01	0.12	1.39	2443	25					-5.68	-11.01
DST-25	4.16	6.71	0.97	2211	32	7.9	34.0	30.9	28.2	-6.18	-11.82
DST-26	4.34	4.67	1.25	1296	57	8.9	35.0	31.9	29.2	-5.91	-9.72
DST-27	4.54	0.41	<d.l.	1028	30	6.4	32.5	29.4	26.7	-5.63	-9.63
DST-28	4.74	3.31	0.42	772	46	8	34.1	31.0	28.3	-5.26	-8.57
DST-29	4.84	4.03	5.13	1549	41	7.3	33.4	30.3	27.6	-5.31	-10.77
DST-30	4.99	0.24	<d.l.	1421	35	6.1	32.2	29.1	26.4	-5.15	-10.59
DST-31	5.09	0.15	1.80	841	41	8	34.1	31.0	28.3	-5.76	-9.91
replicate										-5.72	-9.92
replicate										-5.7	-10.02

Element concentrations and Li isotope compositions were measured in leaching solutions while oxygen and carbon isotope compositions were measured in bulk rock. External analytical uncertainty is 1.2 ‰ for δ^7Li, 0.065 ‰ for δ^{13}C and 0.12 ‰ for δ^{18}O (2σ). δ^7Li_{sw} @10, 25 and 40°C are the seawater compositions calculated using the relationship between the Li isotope fractionation factor and precipitation temperature from Taylor et al. (2018), and temperatures of cap dolostone formation of 10, 25 and 40 °C.

Clim. Past Discuss., https://doi.org/10.5194/cp-2018-119
Manuscript under review for journal Clim. Past
Discussion started: 20 September 2018

Climate of the Past Discussions
Open Access
EGU

Table 4. Model results

Scenario #	T_{lag} (Myr)	T_{carb} (Myr)	Stage duration (Myr)	F_r/ $F_{r,mod}$	δ^7Li_r
1	0	3	15, 0.1, 2.9	0, 50, 5	23, 35, 20
2	1	3	15, 1, 3	0, 3, 1	23, 35, 23
3	1	3	15, 1, 3	0.8, 3, 1	23, 30, 23
4	0	3	15, 0.1, 2.9	0.8, 10, 1	23, 35, 23
5	1	0.3	15, 1, 0.3	0, 3, 2	23, 35, 35
6	1	3	15, 1, 3	0, 3, 5	23, 35, 20

T_{lag}: Delay between end of glaciation and onset of cap carbonate deposition. T_{carb}: Duration of cap carbonation deposition. F_r/ $F_{r,mod}$: riverine Li flux relative to the modern value (10 Gmol/yr), δ^7Li_r: riverine Li isotopic composition. Seawater temperature during cap dolostone deposition: 25 °C. Series of three numbers in the three rightmost columns represent values for stages 1 to 3. Scenarios 1-5: well-mixed ocean; scenario 6: stratified ocean during stage 2.

Clim. Past Discuss., https://doi.org/10.5194/cp-2018-119
Manuscript under review for journal Clim. Past
Discussion started: 20 September 2018

Climate of the Past Discussions
Open Access
EGU

Figure 1

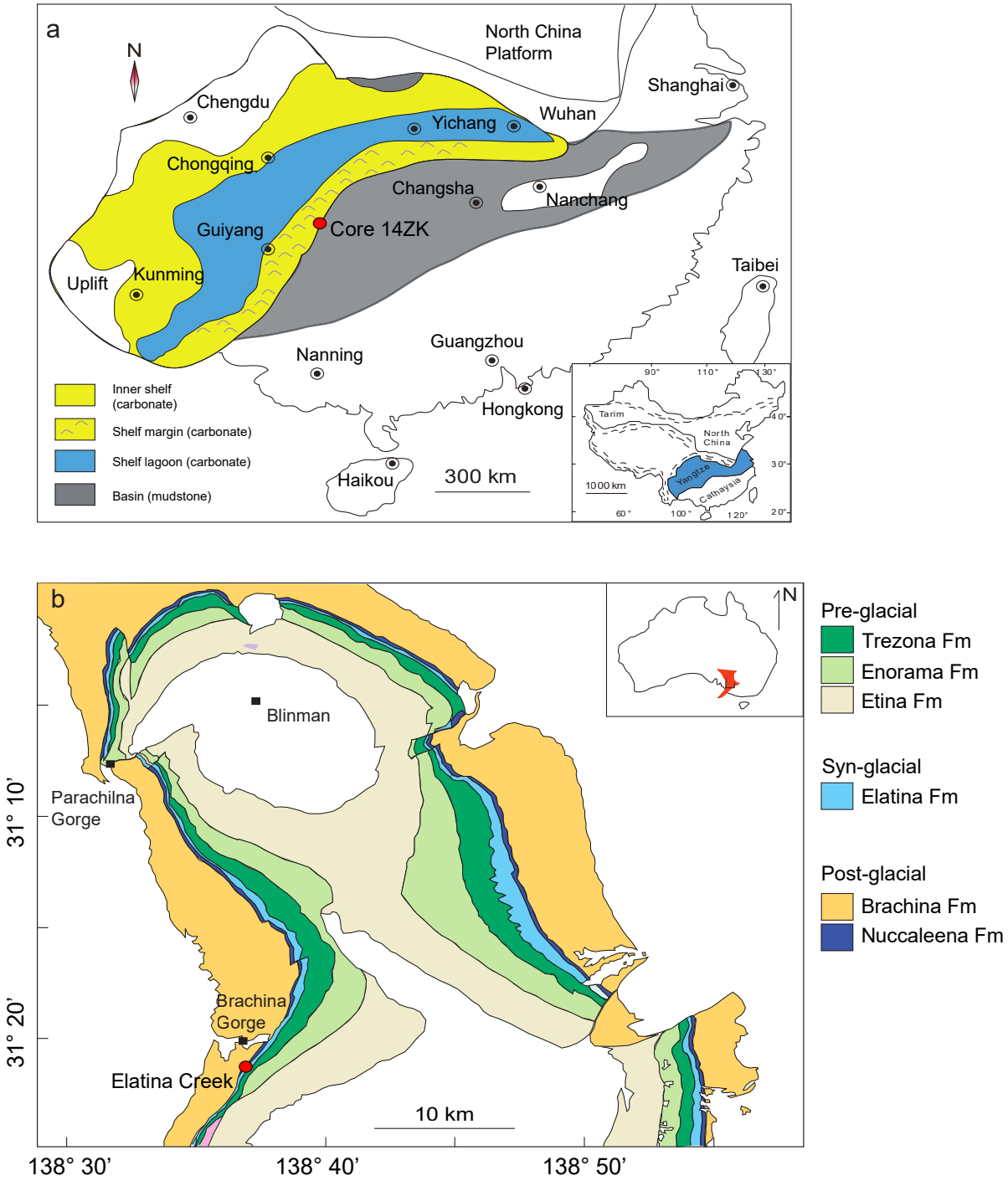

Clim. Past Discuss., https://doi.org/10.5194/cp-2018-119
Manuscript under review for journal Clim. Past
Discussion started: 20 September 2018

Climate of the Past Discussions

Figure 2

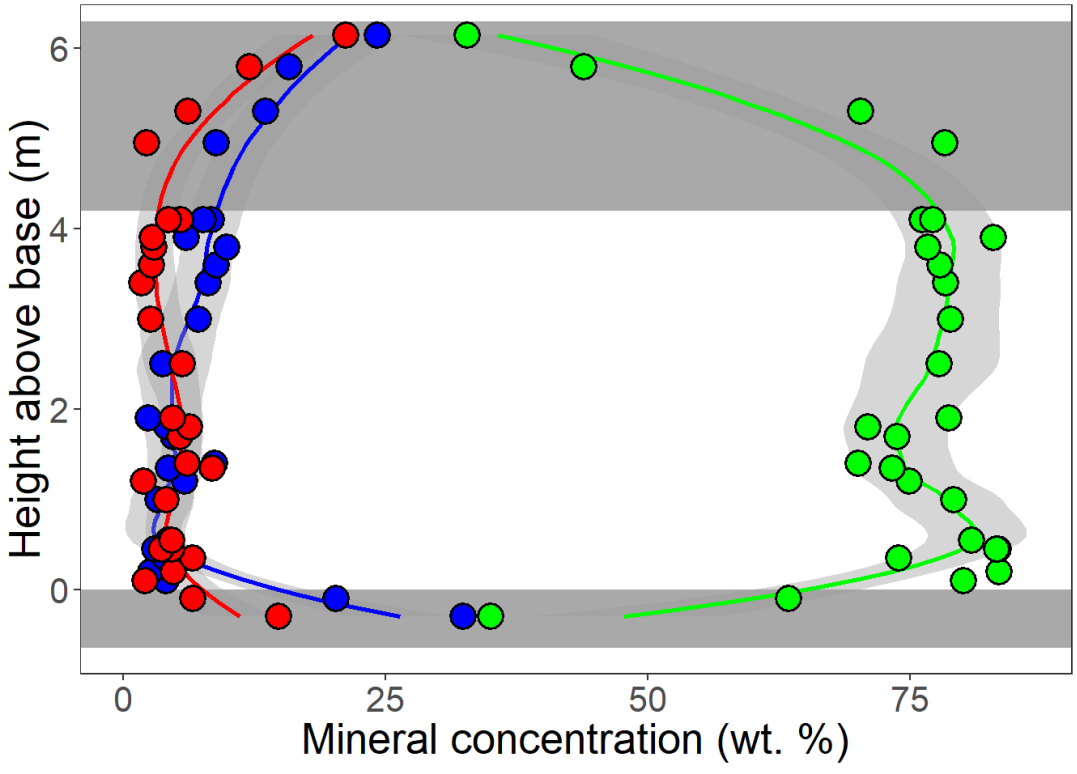

Clim. Past Discuss., https://doi.org/10.5194/cp-2018-119
Manuscript under review for journal Clim. Past
Discussion started: 20 September 2018

Climate of the Past
Discussions
Open Access
EGU

Figure 3

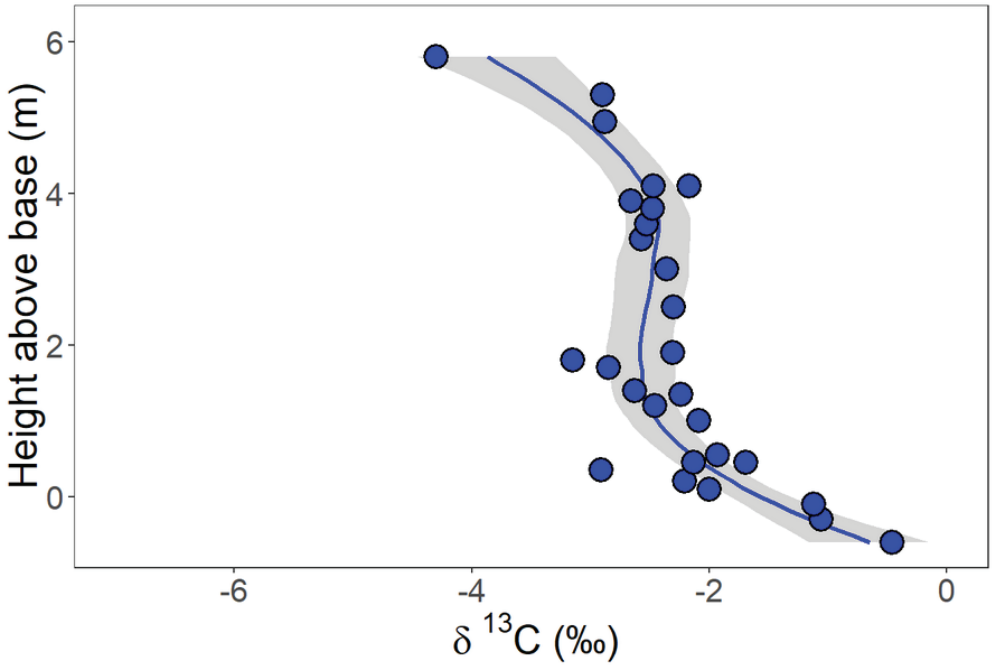

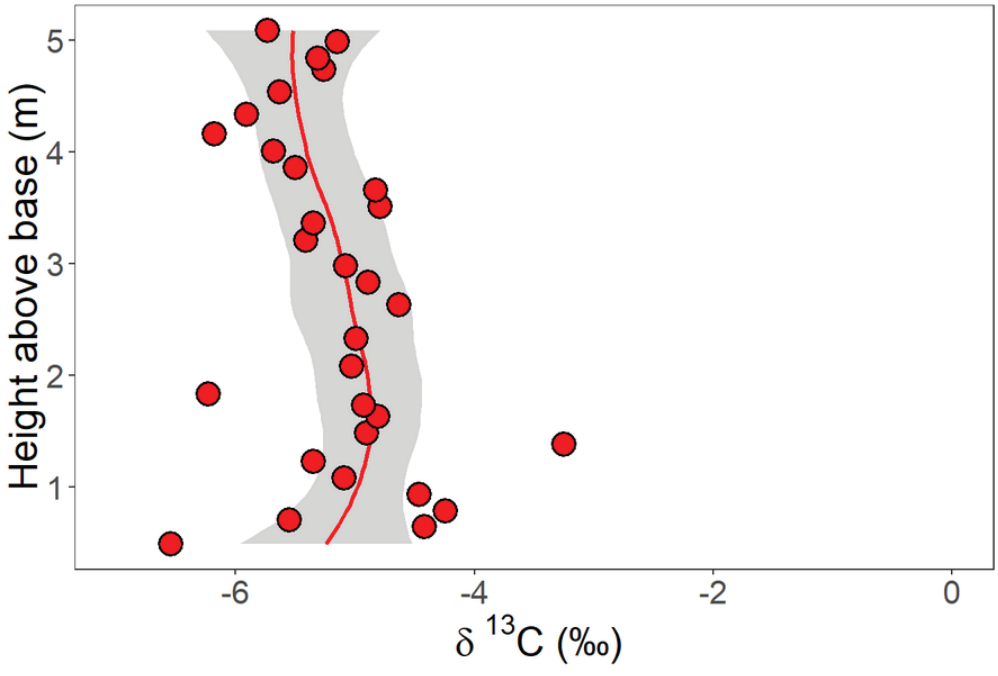

Clim. Past Discuss., https://doi.org/10.5194/cp-2018-119
Manuscript under review for journal Clim. Past
Discussion started: 20 September 2018

Climate of the Past
Discussions
Open Access
EGU

Figure 4

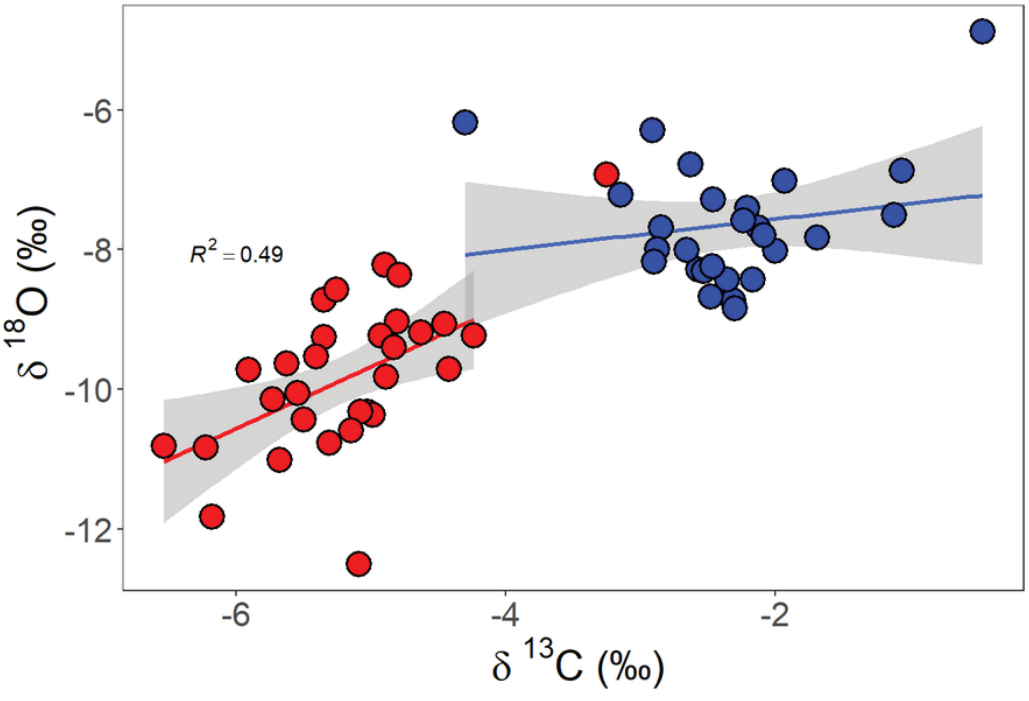

Clim. Past Discuss., https://doi.org/10.5194/cp-2018-119
Manuscript under review for journal Clim. Past
Discussion started: 20 September 2018

Climate of the Past Discussions

Figure 5

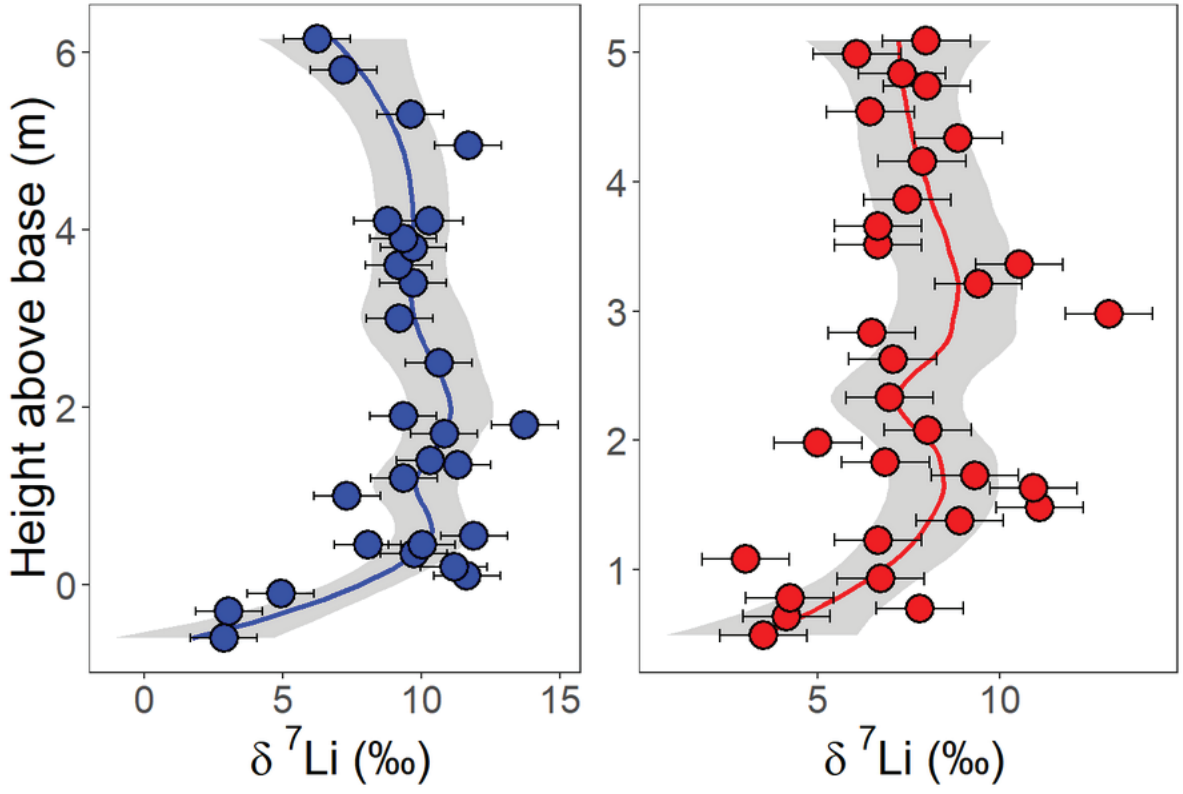

Clim. Past Discuss., https://doi.org/10.5194/cp-2018-119
Manuscript under review for journal Clim. Past
Discussion started: 20 September 2018

Climate of the Past Discussions

Figure 6

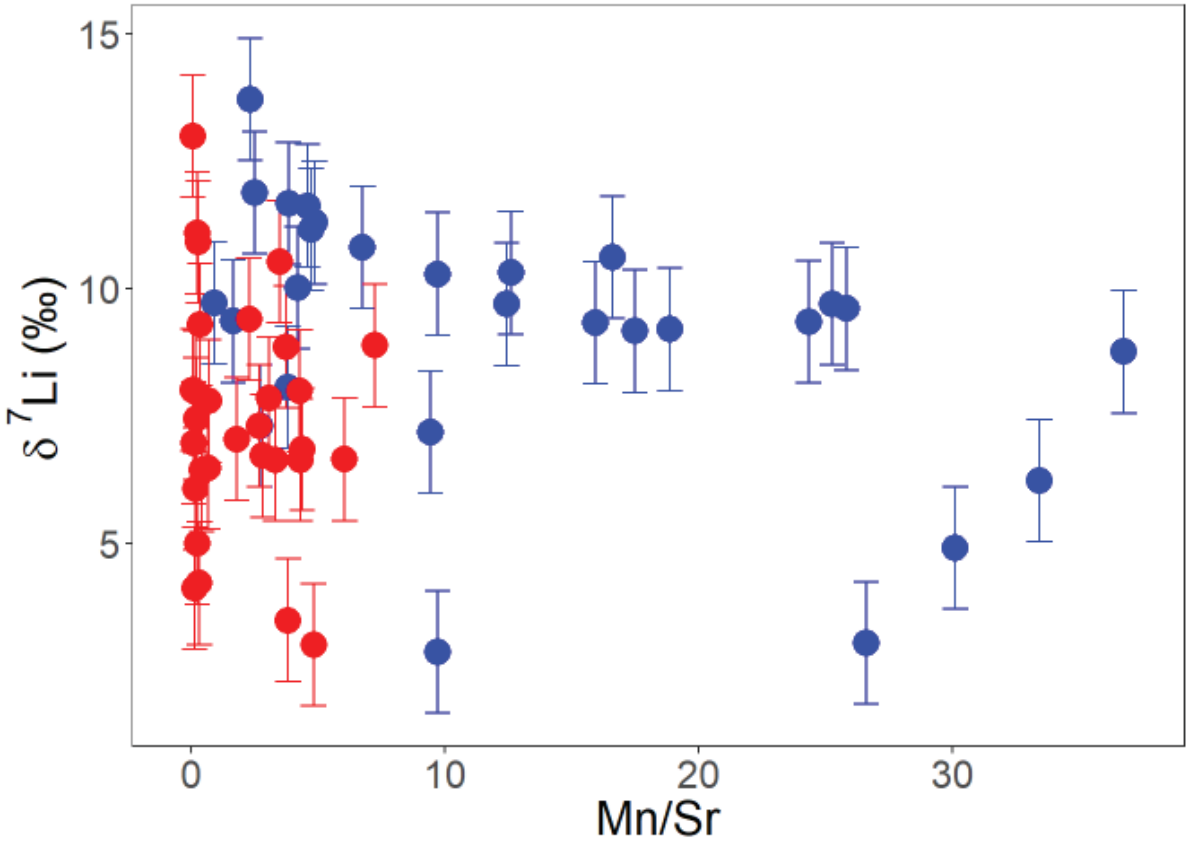

Clim. Past Discuss., https://doi.org/10.5194/cp-2018-119
Manuscript under review for journal Clim. Past
Discussion started: 20 September 2018

Climate of the Past Discussions
Open Access
EGU

Figure 7

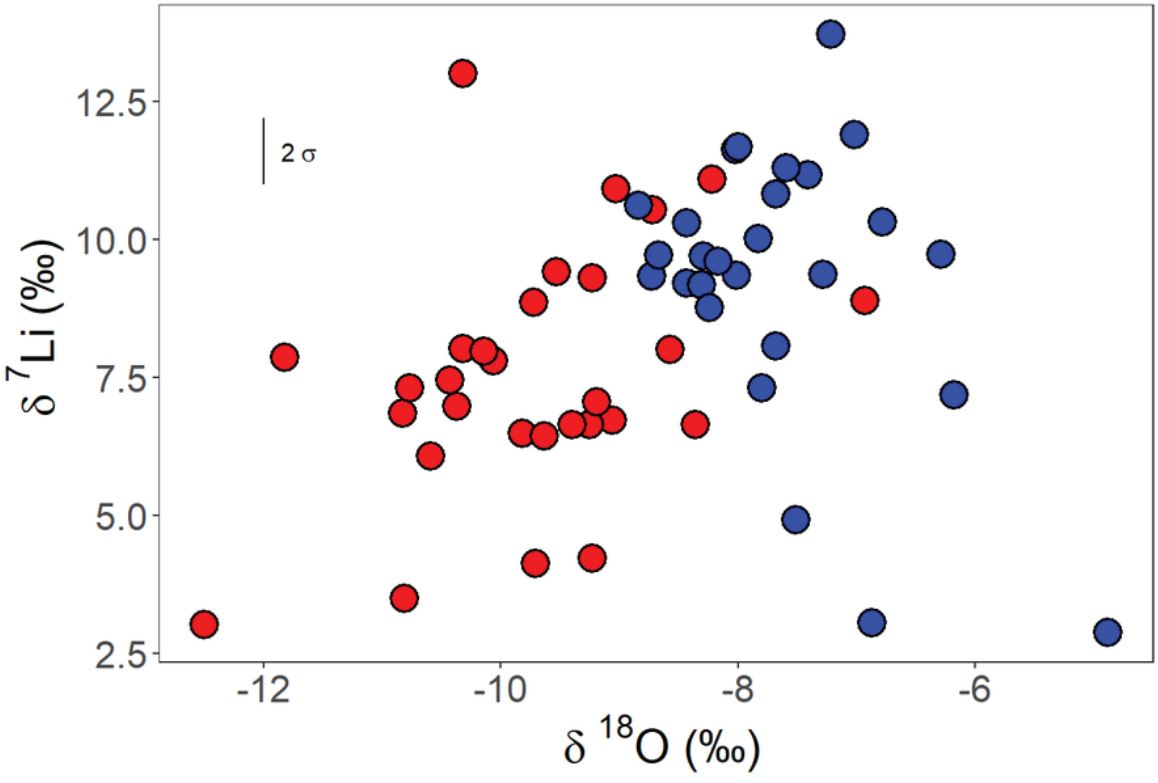

Clim. Past Discuss., https://doi.org/10.5194/cp-2018-119
Manuscript under review for journal Clim. Past
Discussion started: 20 September 2018

Climate of the Past Discussions

Figure 8

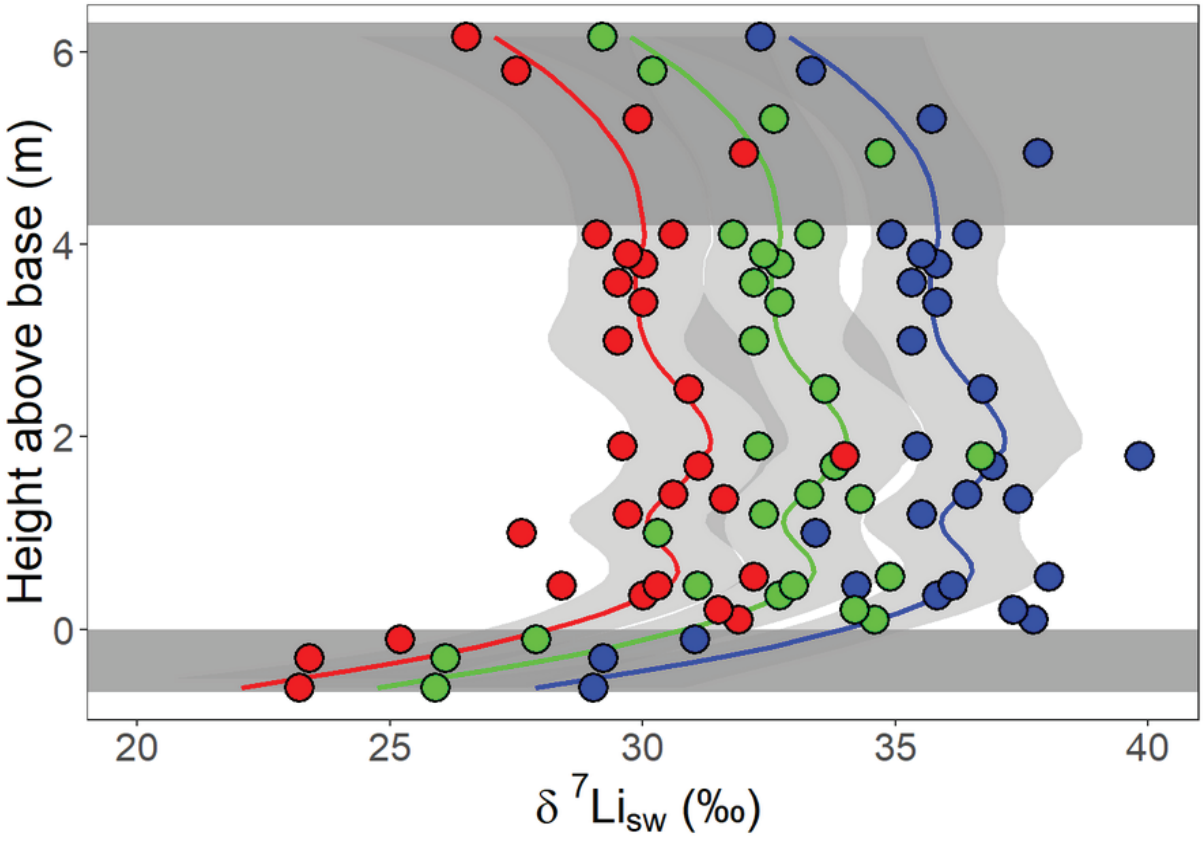

Clim. Past Discuss., https://doi.org/10.5194/cp-2018-119
Manuscript under review for journal Clim. Past
Discussion started: 20 September 2018

Climate of the Past Discussions
Open Access
EGU

Figure 9

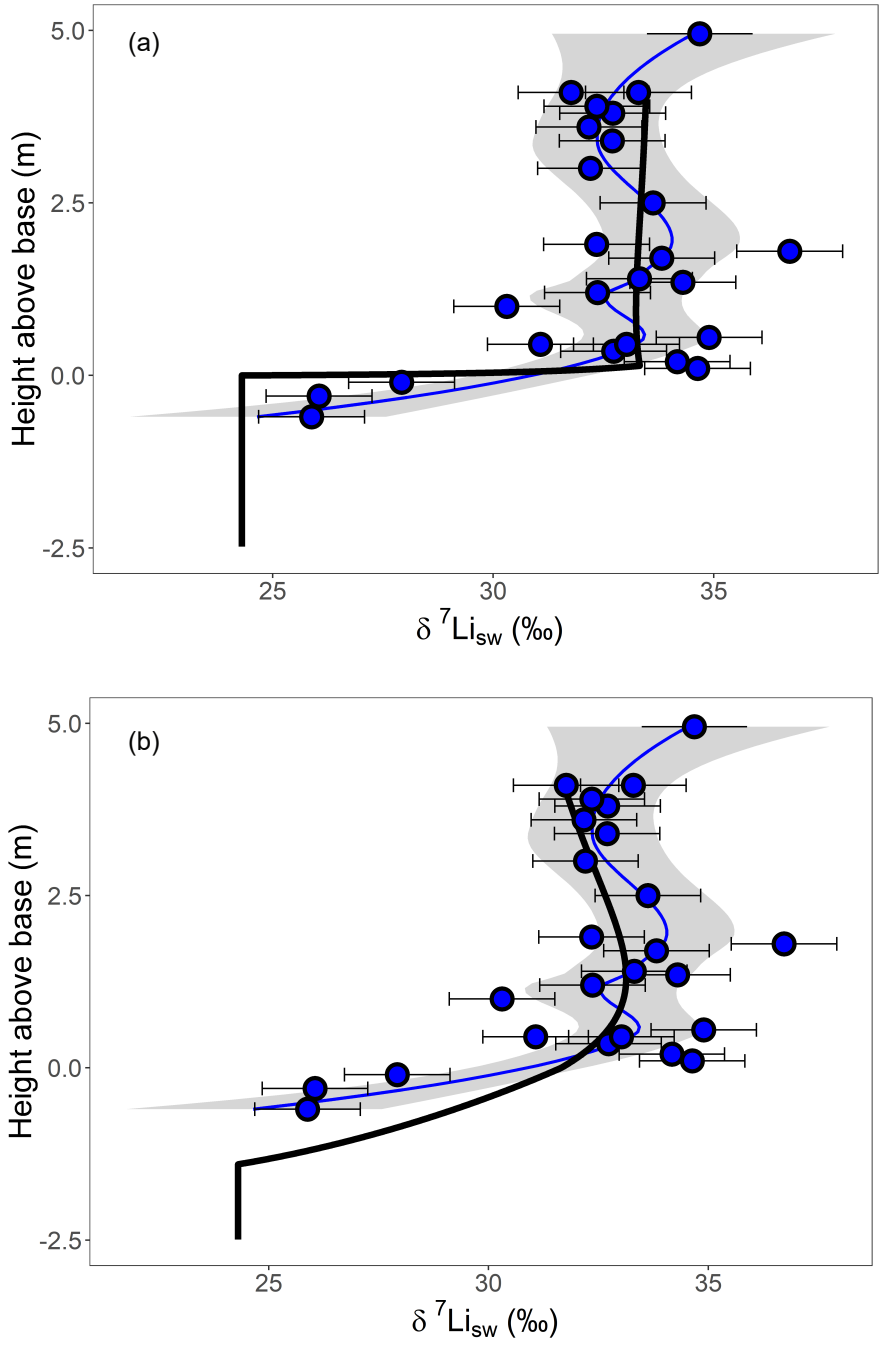

Clim. Past Discuss., https://doi.org/10.5194/cp-2018-119
Manuscript under review for journal Clim. Past
Discussion started: 20 September 2018

Climate of the Past Discussions

Figure 10

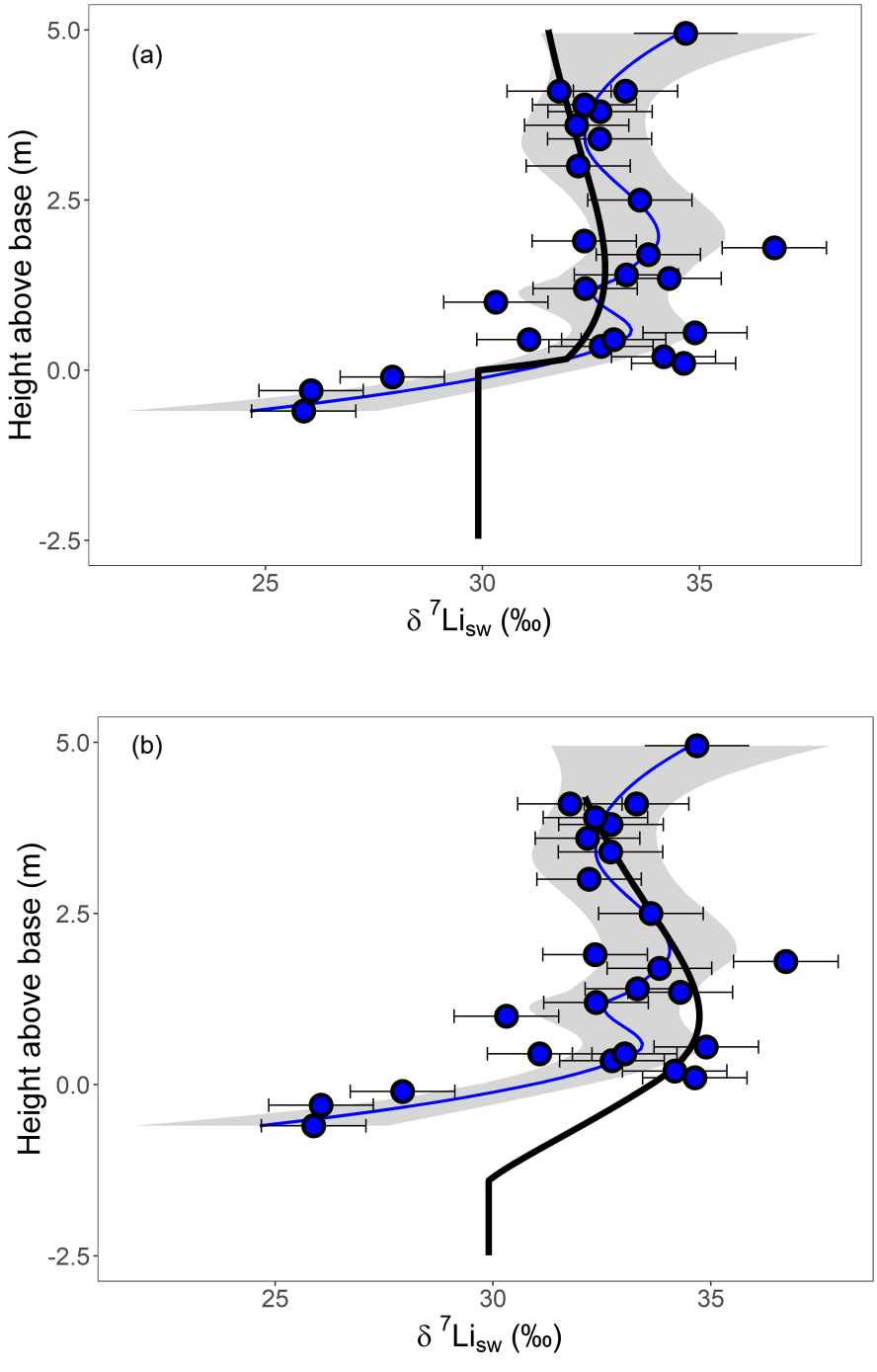

Clim. Past Discuss., https://doi.org/10.5194/cp-2018-119
Manuscript under review for journal Clim. Past
Discussion started: 20 September 2018

Climate of the Past Discussions
Open Access
EGU

Figure 11

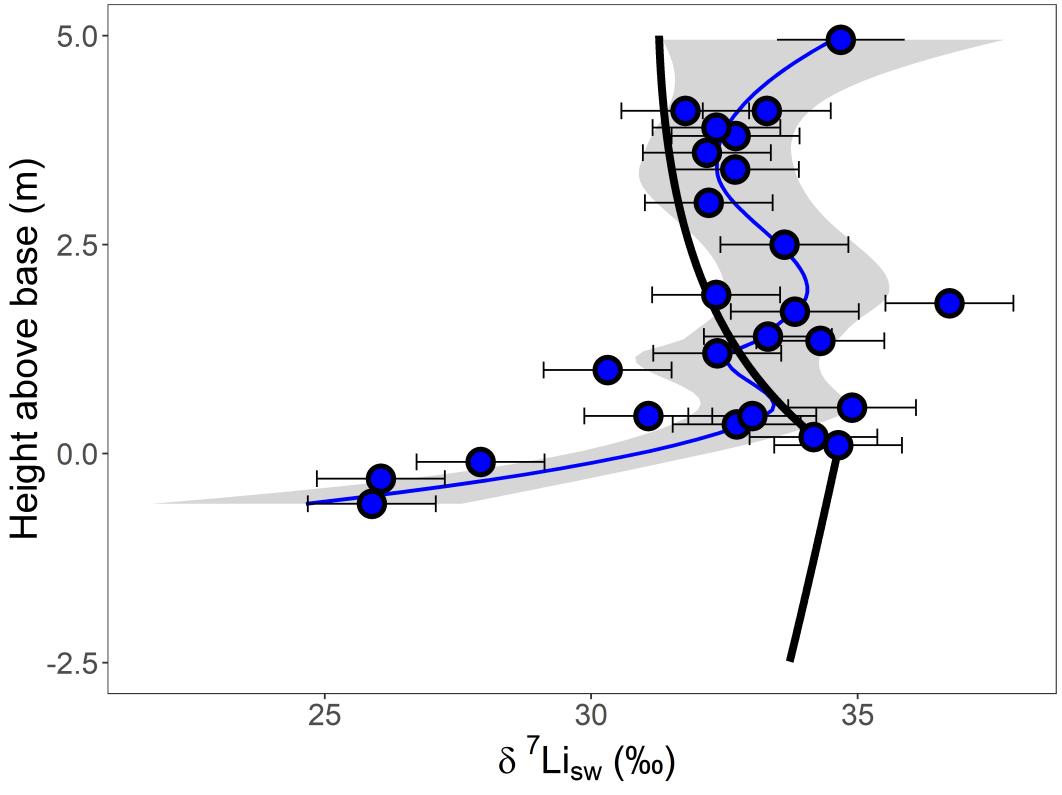

Clim. Past Discuss., https://doi.org/10.5194/cp-2018-119
Manuscript under review for journal Clim. Past
Discussion started: 20 September 2018

Climate of the Past Discussions

Figure 12